

Enhanced Entrained Air Void System Characterization for Durable Highway Concrete

Anthony Torres, PhD and Federico Aguayo, PhD, Principal Investigators
Engineering Technology
Texas State University

SEPTEMBER 2022

Research Project of the National Road Research Alliance
Rigid Technical Team
Final Report NRRRA202204



Technical Report Documentation Page

1. Report No. NRRA202204	2.	3. Recipients Accession No.	
4. Title and Subtitle Enhanced Entrained Air Void System Characterization for Durable Highway Concrete		5. Report Date September 2022	
		6.	
7. Author(s) Anthony Torres, PhD; and Federico Aguayo, PhD		8. Performing Organization Report No.	
9. Performing Organization Name and Address Engineering Technology Texas State University 601 University Dr. San Marcos, TX 78666		10. Project/Task/Work Unit No. Task 8	
		11. Contract (C) or Grant (G) No. No. 1036340	
12. Sponsoring Organization Name and Address Minnesota Department of Transportation Office of Research & Innovation 395 John Ireland Boulevard, MS 330 St. Paul, Minnesota 55155-1899		13. Type of Report and Period Covered	
		14. Sponsoring Agency Code	
15. Supplementary Notes https://www.dot.state.mn.us/research/reports/2022/NRRA202204.pdf			
16. Abstract (Limit: 250 words) The air void system in concrete provides a strong influence on the behavior of cementitious materials in both the fresh and hardened state, especially as it relates to freeze-thaw resistance and deicer scaling. The most common test procedure to characterize the air void system is <i>ASTM C457 – Standard Test method for Microscopical Determination of Parameters of the Air-Void System in Hardened Concrete</i> , which involves microscopic determination of the air content, paste content, air-void size distribution, and spatial dispersion of a sawn concrete sample. This procedure is reliant on the user to make hundreds of critical decisions per sample, which requires significant time, and is potentially subject to human error. Additionally, ASTM C457 provides minimal guidance regarding the exact steps and equipment necessary to prepare a sample for evaluation. The outcome of this research not only provides specific information regarding sample preparation for hardened concrete air void analysis, it also develops an alternative characterization technique that drastically minimizes evaluation time, human error, and increases reliability of key hardened air void characterization parameters. Specific results show on average air void difference of 0.5% and 0.7% between the alternative method versus ASTM C457 Procedure A and B, respectively. The results also show a significant reduction of analysis time from approximately 2 – 4 hours per sample to 15 minutes per sample when using the alternative method.			
17. Document Analysis/Descriptors Air Voids, Characterization, Methods, Durability, Freeze-Thaw		18. Availability Statement No restrictions. Document available from: National Technical Information Services, Alexandria, Virginia 22312	
19. Security Class (this report) Unclassified	20. Security Class (this page) Unclassified	21. No. of Pages 83	22. Price

Enhanced Entrained Air Void System Characterization for Durable Highway Concrete

FINAL REPORT

Prepared by:

Anthony Torres, PhD;
Engineering Technology
Texas State University

Federico Aguayo, PhD
Department of Construction and Civil Engineering
University of Washington-Seattle

September 2022

Published by:

Minnesota Department of Transportation
Office of Research & Innovation
395 John Ireland Boulevard, MS 330
St. Paul, Minnesota 55155-1899

This report represents the results of research conducted by the authors and does not necessarily represent the views or policies of the Minnesota Department of Transportation or Texas State University. This report does not contain a standard or specified technique.

The authors, the Minnesota Department of Transportation, and Texas State University do not endorse products or manufacturers. Trade or manufacturers' names appear herein solely because they are considered essential to this report.

ACKNOWLEDGMENTS

The authors of this report would like to acknowledge the National Road Research Alliance (NRRRA) and the Technical Advisory Panel (TAP) members for their support and advice. The authors would also like to thank the technical liaison for his time, guidance, and support during this project; Tom Burnham, MnDOT. The following is a list of the TAP members that the authors would also like to thank.

- Bernard Izevbekhai, MnDOT
- David Lim, Caltrans
- Maria Masten, MnDOT
- Angel Mateos, UC-Berkley
- Peter Taylor, Iowa State U. CPTech Center
- Brett Trautman, MoDOT

The research team sincerely acknowledges the contribution of the students, faculties, and staff of the Texas State University who helped at different phases of this project.

TABLE OF CONTENTS

CHAPTER 1: Introduction	1
1.1 General	1
1.2 Background Information.....	1
1.3 Goals and Objectives	3
CHAPTER 2: Research Methodology	5
CHAPTER 3: Fresh and Compressive Strength Results	7
CHAPTER 4: Hardened Concrete Sample Preperation Discussion and Recommendations	8
4.1 Development and Discussion of Preperation Steps	8
4.1.1 Sample Cutting	8
4.1.2 Sample Polishing	11
4.1.3 Contrast Enhancement of Hardened Concrete Samples	13
CHAPTER 5: ASTM C457 Sample Characterization	17
5.1 Methodology	17
5.2 ASTM C457 Results	18
CHAPTER 6: Alternative Air Void Characterization Method Testing and Development	24
6.1 Introduction To The Alternative Method	24
6.2 alternative Digital Optical Microscope Method	24
6.2.1 Hardware.....	24
6.2.2 Software Capabilities.....	25
6.3 Brief summary of alternative analysis procedures	31
6.4 Calculations and Results	31
6.4.1 Calculations	31
6.4.2 Results	33
CHAPTER 7: Results Analysis and Comparison	38

7.1 Methodology	38
7.2 Final Results Analysis and Comparisons	38
CHAPTER 8: Conclusions and Recommendations	46
8.1 Introduction	46
8.2 Major Conclusions and recommendations	46
8.3 Methodology for Implementation	47
8.4 Steps and Approach for Evaluating Benefits (Both Quantitative and Qualitative)	47
8.4.1 Quantitative Result Benefits	47
8.4.2 Qualitative Results Benefits	48
8.5 Discussion of Next Steps for Implementation	48
8.5.1 Considerations Related to the Alternative Hardened Air Void Analysis Method	48
8.5.2 Considerations on General Fresh and Hardened Air Void Analysis	49
REFERENCES	51
Appendix A	1
A.1 Saw Cutting Materials, Equipment, and Procedures	2
A.1.2 Saw Cutting Procedures	2
A.1.3 Polishing Materials and Equipment	3
A.1.4 Polishing Procedures	3
A.1.5 Contrast Enhancement Materials and Equipment	5
A.1.6 Contrast Enhancement Procedures	6
A.2 Alternative Air Void Characterization Equipment and Procedures	10
A.2.1 Alternative Air Void Characterization Method Equipment	10
A.2.2 Alternative Air Void Characterization Procedures	10

LIST OF FIGURES

- Figure 2.1 Particle size distribution for river gravel and river sand.5
- Figure 4.1 Wet masonry saw from Humboldt.8
- Figure 4.2 The two sawblades investigated in this study.....9
- Figure 4.3 Using a c-clamp to mount the concrete sample to the saw table.....9
- Figure 4.4 Masonry saw blade cut quality.10
- Figure 4.5 Diamond cut off blade cut quality.....11
- Figure 4.6 Stuers Abramin Auto-Polisher.11
- Figure 5.1 Linear Traverse Machine.17
- Figure 5.2 Control (2% Target) Hardened Air Void Comparison.20
- Figure 5.3 Low Air (3-5% Target) Hardened Air Void Comparison.20
- Figure 5.4 Medium Air (5-7% Target) Hardened Air Void Comparison.21
- Figure 5.5 High Air (>8% Target) Hardened Air Void Comparison.21
- Figure 6.1 Keyence – VHX 7000 Series Digital Optical Microscope.24
- Figure 6.2 Stitched and Measured Sample.26
- Figure 6.3 Individual Air Void Analysis Display.27
- Figure 6.4 Object Measurement Information.28
- Figure 6.5 Example Screen Shot of Measurement Information.29
- Figure 6.6 Split Window View on Keyence Microscope.30
- Figure 6.7 Screenshot of Excel™ Specific Surface and Spacing Factor Calculator.32
- Figure 7.1 Control (2% Target) Hardened Air Void Comparison.38
- Figure 7.2: Low Air (3-5% Target) Hardened Air Void Comparison.39
- Figure 7.3: Medium Air (5-7% Target) Hardened Air Void Comparison.39
- Figure 7.4: High Air (>8% Target) Hardened Air Void Comparison.40
- Figure 7.5: Comparison Between Alternative Method vs. Linear Traverse Method (ASTM C457 Procedure A).....41

Figure 7.6: Comparison Between Alternative Method vs. Modified Point Count Method (ASTM C457 Procedure B).....	42
Figure 7.7: Average Spacing Factor Results for the Alternative Method and ASTM C457.....	43
Figure 7.8: Average Specific Surface Results for the Alternative Method and ASTM C457.....	44
Figure 8.1 Machine Learning Process for Hardened Air Void Analysis.....	50
Figure A.1 Concrete cylinder mounted to wet saw.	2
Figure A.2 Example of Drawn Grid with Crayon.....	3
Figure A.3 Example of An Incomplete Polish.	4
Figure A.4 Rubber Roller Loaded with Ink.	6
Figure A.5a-c Applying Ink to Polished Sample With Rubber Roller.	7
Figure A.6a-i Enhanced Air Void Contrast Procedure.	8
Figure A.7a-b Mineral Oil Application.	9
Figure A.8 Completed Concrete Surface for Hardened Air Void Analysis.....	10
Figure A.9 Screenshot of VHX Software User Window with a Fully Stitched Concrete Sample.	11
Figure A.10 Example of the Measuring Preview Window.....	13
Figure A.11 Example of the Area Specified Circle Procedure.	14
Figure A.12 Example of Eliminate Grains Pop-up Window.	15
Figure A.13 Example of Auto Area Measurement Results.	16

LIST OF TABLES

- Table 2.1 Concrete Mixture Proportions6
- Table 3.1 Fresh and Compressive Strength Results7
- Table 5.1 ASTM C457 Procedure A and B Results.....19
- Table 6.1 Initial Hardened Air Void Analysis Results Completed with the Keyence – VHX 7000
Microscope.....34
- Table 6.2 Pore Type and Function Related to Freeze-Thaw Durability [35].35
- Table 6.3 Secondary Hardened Air Void Analysis Results Completed with the Keyence – VHX 7000
Microscope.....37
- Table A.1 Saw Cutting Materials and Equipment2
- Table A.2 Polishing Materials and Equipment.3
- Table A.3 Contrast Enhancement Materials and Equipment.5
- Table A.4 Equipment used to Complete an Alternative Hardened Air Void Characterization.....10
- Digital Optical Microscope Component.....10
- VHX 7000 Controller.....10
- Fully Integrated Camera10
- Console10
- Focus View Motorized XYZ Stage – (100mm range of motion)10
- 20-100X FI Lens10
- 100-500X FI Lens10

LIST OF ABBREVIATIONS

AEA: Air-Entraining Admixtures

ASTM: American Society for Testing and Materials

C-S-H: Calcium silicate hydrate

NRRA: National Road Research Alliance

p/A: Paste-Air Ratio

SAM: Super Air Meter

SCM: Supplementary Cementitious Materials

SSD: Saturated Surface Dry

w/c: water to cement ratio

w/cm: water to cementitious material ratio

EXECUTIVE SUMMARY

The air void system in concrete provides a strong influence on the behavior of cementitious materials in both the fresh and hardened state, especially as it relates to freeze-thaw resistance and deicer scaling. The most common test procedure to characterize the air void system is *ASTM C457 – Standard Test method for Microscopical Determination of Parameters of the Air-Void System in Hardened Concrete*, which involves microscopic determination of the air content, paste content, air-void size distribution, and spatial dispersion of a hardened concrete sample. This procedure is reliant on the user to make hundreds of critical decisions per sample, which requires significant time, and is potentially subject to human error. Additionally, ASTM C457 Procedure C requires significant sample preparation, including lapping, polishing, and dyeing which is laborious and time consuming. Due to this drawback, most state agencies do not perform this test and generally rely on fresh concrete air content as per ASTM C231, which may not always be reliable in approving a concrete mixture for freeze-thaw and/or deicer scaling resistance. Therefore, there exists a need to develop a method to fully characterize the air void system in hardened concrete that is more reliable, less time consuming, cost effective, and easy to complete.

This study, supported by the National Road Research Alliance (NRRRA), is intended to develop and assess an alternative test procedure to characterize the entrained air void system for hardened concrete. The procedure utilized a digital optical microscope with onboard counting and measuring software, which uses sophisticated measurements to determine the hardened air void parameters of a prepared concrete sample. Also investigated in this study was further insight as to how to properly polish and contrast enhance a hardened concrete sample, with particular emphasis on cost and sample prep time minimization.

The research in this document has the benefit to provide an alternative hardened air void characterization technique to that of ASTM C457, benefiting multiple state agencies within the NRRRA. The alternative characterization technique has the capability to not only produce accurate key hardened air void system information, but it also has a significant quality of life improvement for the operator compared to current ASTM procedures. The alternative technique not only provides consistent, accurate, and reliable results as compared to ASTM C457, but the entire process takes on the order of 15 minutes versus the 2 – 4 hours, is partially automated, extremely repeatable from user-to-user and lab-to-lab, and the software is extremely intuitive to learn/understand. Through the development of the alternative characterization technique, many discoveries were made regarding the development (cutting, polishing, contrast enhancement, etc.) of the hardened concrete sample and are discussed in this report. Therefore, this report also includes suggestions and advice regarding equipment, materials, methods, and techniques to help prepare a hardened concrete sample for evaluation following any of the three ASTM C457 procedures or the alternative method as outlined in this report.

The entire research work was divided into eight different tasks. Task 1 provided information regarding initial estimates of expected research benefits, documentation of the proposed methodology, and potential implementation steps. Task 2 focused on producing concrete and obtaining fresh properties (slump, unit weight, air content, and Super Air Meter (SAM) number) as well as 7 and 28-day compressive strengths. Task 3 aimed at developing a sample preparation procedure to both polish and

contrast enhance the hardened concrete samples. This task investigated multiple methods and procedures to saw cut, polish (with various types and size of polishing pads), and contrast enhance the samples, in which all steps were assessed for quality and time required. Task 4 focused on obtaining baseline ASTM C457 Procedure A (Linear Traverse Method) and Procedure B (Modified Point and Count Method) data on the prepared hardened concrete samples from Task 3. Task 5 discussed the capabilities of the alternative method using a digital optical microscope, including the procedures, calculations, time to complete, and results. Task 6 contained a more comprehensive comparison and discussion of the alternative method results as they compare to both ASTM C457 Procedure A and B. Lastly, Task 7 was a final technical memorandum detailing the methodology, steps and approaches to both evaluate the benefits and implement the alternative method, which also included a discussion of the possible next steps in the evolution of this research. Task 8 involved compilation of the final summary report.

Some key findings from the above tasks are as follows:

1. All concrete mixtures produced in this investigation contained as expected fresh and compressive strength data, relative to the four target air contents investigated.
2. Various hardened concrete sample preparation trials were investigated regarding techniques, materials, equipment, etc. Through these trials various discoveries related to the preparation of the hardened concrete sample for evaluation are as follows:
 - Two concrete saw blades were investigated, and it was discovered that a diamond cut off blade produces superior saw cuts on the concrete cylinders, which will significantly reduce the subsequent polishing steps. This was compared to a conventional masonry saw blade.
 - Regarding sample polishing, two polishing mediums were investigated and it was discovered that diamond metal backed polishing discs last longer and reduce the polishing time significantly as compared to traditional silicon carbide paper polishing discs.
 - Regarding the polishing sequence, various grit sizes and corresponding durations were investigated. It was discovered that with the samples investigated in this study, the first polishing step using the coarsest polishing medium is the most crucial step in producing a suitable surface for further analysis. Through this discovery it was determined that subsequent polishing is not necessary required to determine hardened concrete air void parameters with either ASTM C457 or the alternative method.
 - If a hardened concrete sample requires contrast enhancement, using a water soluble black acrylic ink and a rubber roller is preferred over a black marker. Additionally, the preferred white powder used to fill the air voids in the sample is barium sulfate.
3. The results showed an average hardened air void difference of 0.5% and 0.7% between the alternative hardened air void analysis method and ASTM C457 Procedure A and Procedure B, respectively.
4. The results showed an average air content difference of 0.5% between the alternative hardened air void analysis method and the fresh air content determined with ASTM C231.

5. The results also showed a reduction of time: From an estimated 2 - 4 hours/sample (ASTM C457) down to an estimated 15 minutes/sample (alternative method).

CHAPTER 1: INTRODUCTION

1.1 GENERAL

The impact of the air void system in hardened concrete depends on the total volume, size, and dispersion of the air voids in the concrete system, as well as their compatibility with various material properties. Properties affected by the air void system include workability, cohesion, density (fresh and hardened), strength, finish ability, mixture constituents, and freeze-thaw resistance. The most important of these, in terms of highway concrete, for long-term performance is the resistance to freeze-thaw durability. To effectively provide freeze-thaw resistance, the air void system must have a total volume of empty air voids that equals or exceeds the volume of water or ice not accommodated by space in the capillary pore system [1]. Additionally, the air voids must be dispersed throughout the cement paste so that nearly all of the paste is within an air-void system zone of influence [2 – 10]. The most common method for studying the entrained air void system in hardened concrete is ASTM C457 – “Standard Test Method for Microscopical Determination of Parameters of the Air-Void System in Hardened Concrete” [11]. This method, initially proposed by Brown and Pierson [12], consists of polishing a hardened concrete sawn sample and placing it under a microscope. The operator systematically makes measurements by counting the air voids that come into view. Statistical estimates are produced from the measurements that define the air content, paste content, air-void size distribution, and spatial dispersion. Today, there are three methods described in ASTM C457 (2016): i) the Rosiwal linear traverse technique (Procedure A); ii) the modified point-count method (Procedure B); and iii) the contrast-enhanced method (Procedure C). Although ASTM C457 is a standard test method for characterizing the entrained air void system in concrete, some significant sources of variability and uncertainty still exist in the test results. One major source of variability in Procedure A and B is that multiple human judgment calls are made (on the order of hundreds) and that both procedures could completely overlook air voids, simply by the nature of the procedure. The current procedures can be inherently biased based on the subjective nature of the operator. Therefore, there is a need to develop an alternative hardened concrete air void characterization method that reduces the inherent variability, subjectivity, and uncertainty with ASTM C457.

1.2 BACKGROUND INFORMATION

The ability of concrete to survive a cold and wet environment is primarily dependent on the air void system in the hardened concrete [13]. This is why it is extremely important to accurately and quickly characterize the air void system as promptly as possible. The formation and source of pores in a hydrated cement paste system has a strong influence on the freeze-thaw resistance. Calcium silicate hydrate (C-S-H) is a principal product of cement hydration and Powers [6] recognized that this product determines the properties of cement paste. The porosity of C-S-H is about 25%, due to the presence of pores, which are known as gel pores, with a typical size of a few nanometers [14]. Because of the pores small size water cannot freeze inside them at typical temperatures, although the water in them may be supercooled [7]. During hydration, the voids left behind as the mixing water is removed from the system are known as capillary voids [15]. The sizes of these capillary pores range from approximately 5 nm to

about 1 μm . The volume of capillary pores primarily depends on both the degree of hydration and the original water to cementitious material (w/cm) ratio [8, 14 – 17]. Air voids in hardened cement paste can be considered as either entrapped or entrained. Entrapped air voids occur due to insufficient consolidation. These air voids are typically greater than 3/64 in. (1 mm) in size and are irregular in shape [11]. Entrapped air voids are typically isolated from other entrapped air voids and provide no benefit to the concrete [7]. Entrained air voids are typically 10 to 1,000 μm in diameter and are mostly spherical. Entrained air voids are discrete and uniformly distributed, and therefore have little effect on concrete permeability [13].

Unlike most materials, which become denser during freezing, water expands and becomes less dense when the temperature falls below 32°F. The freezing point of water inside concrete pores depends on the pore sizes, the internal pressure, and the presence of solutes. At higher pressures (> 1 atm), the freezing temperature decreases. The presence of solutes such as K⁺, Na⁺, Ca²⁺, and Cl⁻ in water also depress the initial freezing point [18]. The damage due to freezing action is mainly dependent on the degree of saturation [19]. Damage is unavoidable if the critical degree of saturation of approximately 86% for all of the voids is reached [20]. The following mechanisms are believed to be primarily responsible for freeze-thaw deterioration in concrete [14, 21]:

- Hydraulic pressure generated by freezing in capillaries.
- The diffusion of supercooling gel water into capillaries after freezing.
- Osmotic pressures resulting from the partial freezing in capillaries of solutions that have local concentration differences.
- Differential strains due to localized shrinkage and swelling.

All of the mechanisms are influenced by the ability of fluids to travel through the system, as well as the saturation of the pores. It is difficult for water to penetrate spherical air voids through capillary action due to the nature of surface tension forces; however, external pressures in the pore system may drive fluids into an air void. Damage, then, is significantly influenced by the fluid transport characteristics of the system, as well as the size, shape, and connectivity of the pores [13].

Total air content is defined as the total volume of air voids expressed as a percentage of the bulk volume of concrete. This parameter has been the basis of acceptance testing since the AASHTO T152/ASTM C231 [22] test method was developed. Despite the fact that the critical parameter is the spacing factor, total air content was a satisfactory measure because the correlation between the two parameters was good. With changes to system chemistry using different materials, this correlation has been diminished, increasing the need to measure other parameters that indicate potential durability, such as the SAM number [22, 23]. Powers [5] suggested that air voids perform two functions in concrete: limit the hydraulic pressure in the paste during the early age of freezing, and limit the formation of ice bodies. Based on the first function, the space between air voids, also expressed as the spacing factor, becomes the most important factor because, as water expands with decreasing temperatures (below ~39°F), the water has to flow through saturated pores to find empty air voids before it freezes. Even with the same air content, the spacing factor can be very different between mixtures. Clustering is a phenomenon in which entrained air bubbles preferentially collect around aggregate particles. This clustering reduces the

bond between the paste and the aggregate [1, 23, 24], and so the phenomenon has the potential to reduce compressive strength [25]. However, Riding et al. [26] reported no correlation between clustering and strength. Regardless, a system of small, stable bubbles close together is desirable to provide a sufficient freeze-thaw resistance for concrete exposed to cold, wet weather. Compared to capillary pores, spherical voids are much more difficult to fill with water under capillary action. This has the effect of reducing the degree of saturation of the system at any given time. Unsaturated bubbles provide a space into which expanding water and ice can move, without incurring pressures within the hydrated cement paste, which can ultimately crack and fail the concrete. The bubbles need to be close together to reduce the distance that expanding water has to travel, and they need to be small to reduce the impact on the mechanical properties of the mixture. The principal objective of using air-entraining admixtures (AEAs) in concrete is to provide and stabilize an air-void structure that is able to protect concrete from the deterioration brought by freezing and thawing. AEAs are surfactants that are readily adsorbed at air-water or solid-water interfaces and serve as bubble stabilizers. There are currently two explanations as to how the air-void system forms during mixing. One explanation is that, during concrete mixing, air layers are trapped between the folding surfaces of the concrete, and the fine aggregate acts as a “three-dimensional screen” to hold air bubbles within the network of particles [1, 5, 24]. Powers [5,6] described another process in which air bubbles are formed in a vortex as the mixture is stirred. Mixing provides the energy to build the interface between air and liquid in large air voids and then splits the large voids into smaller bubbles.

The most commonly tested parameters for expressing the characteristics of an air-void system in hardened concrete are total volume of air, specific surface, and spacing factor. Conventionally, the average chord length of voids is used to calculate the specific surface and spacing factor. With more recent technologies, such as flatbed scanners used with bubble counter analysis software [1] and x-ray imaging [24], analysis of air-void connectivity, clustering, and spatial distribution is also possible. Currently, most existing test methods only measure air voids a few microns long and longer. Based on these measurements, it is widely accepted that the spacing factor of an air-void system should typically be less than 0.008 in. (0.20 mm) to provide the greatest protection against freeze-thaw damage [27]. However, recent studies have found that much smaller air voids and spacing factors also play an important role in freeze-thaw durability performance [20, 21, 23]. The ASTM C457 microscopical method has long been a reference method in determining the spacing factor and specific surface of air voids in concrete. The linear traverse and point count techniques use a microscope and user interpretation to evaluate an air-void structure. Although this is the most common practice to characterize the hardened air void system of concrete samples, it is the most tedious and susceptible to user/operator error.

1.3 GOALS AND OBJECTIVES

The goals and objectives of this study are the following:

1. Develop an alternative hardened air void test method that captures all air voids in the sample and does not rely on operator judgment calls.
2. Produce a list of procedures required to produce the hardened air void parameters.

3. Provide further insight and possibly reduce the time required to prepare a hardened concrete sample for air-void system evaluation.
4. Compare and discuss the results of the alternative analysis to the Procedure A and B of ASTM C457.

CHAPTER 2: RESEARCH METHODOLOGY

In order to properly develop and compare the alternative characterization method, multiple samples were produced and analyzed. For this investigation one w/c was used (0.50) along with four target air void percentages (control at 2%, low at 3 – 5%, medium at 5 – 7%, and high at >8%). Two different brands of saw blades were investigated. Two different polishing mediums were investigated (silicon carbide and diamond) at 6 different polishing pad grit sizes (260µm, 125µm, 70µm, 30µm, 15µm, and 6µm). Six different polishing pad grit sizes were used in order to determine if the degree of polish has any effect on the alternative technique.

Regarding the specific concrete constituents, a Type I/II ordinary portland cement was used for all mixtures. A locally available River Gravel (#67 grading) and River Sand that meets ASTM C33 requirements were used in all mixtures. The particle size distribution of these two aggregates can be seen in Figure 2.1.

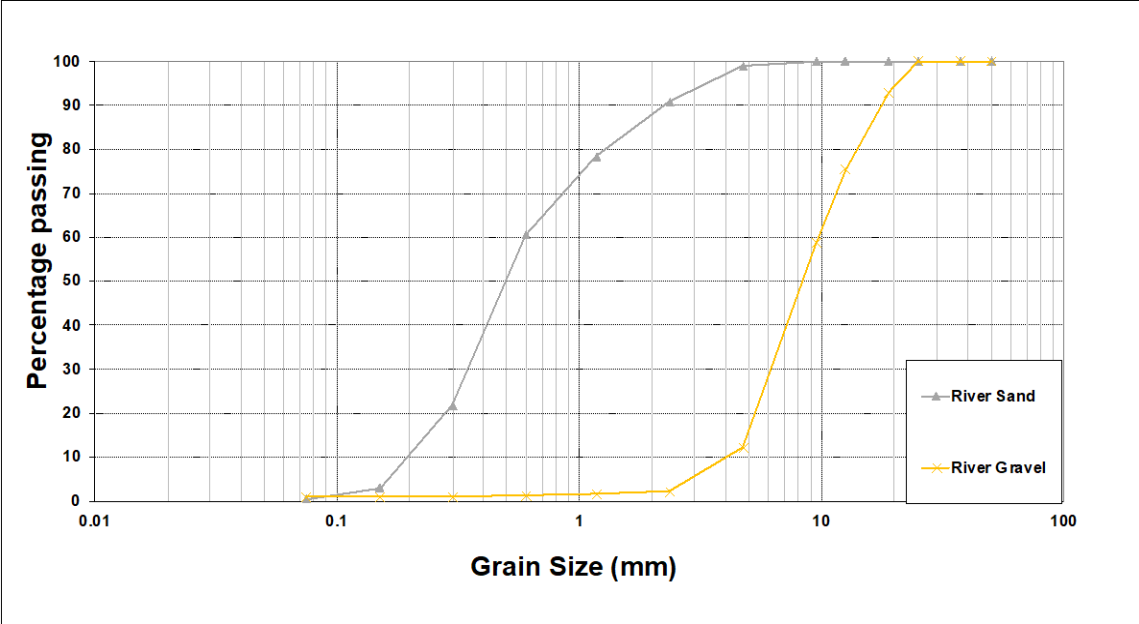


Figure 2.1 Particle size distribution for river gravel and river sand.

Only, one AEA was used in this study in order to provide consistent results, which allowed the study to focus on the new characterization method. A locally available AEA was used, which meets ASTM C260.

Four straight cement concrete mixtures, with no supplementary cementitious materials, were produced in this study with the aforementioned materials. The mixtures were simple highway pavement mixtures aimed solely at producing various entrained air contents. A consistent slump of 3-5” was targeting to create similar workability between all mixtures. The air entraining dosages were added at various ranges sufficient enough to provide a low (3-4%), moderate (5-7%), and high (> 8%) fresh air contents in the produced mixtures. A non-air entrained mixture was also included as a reference in the study (control: 2%). Table 2.1 shows the mixture proportions of the four mixtures produced.

Table 2.1 Concrete Mixture Proportions

Material	Control	Low Air	Medium Air	High Air
Type I/II Cement (lbs/yd ³)	565	565	565	565
Water (lbs/yd ³)	282	282	282	282
River Gravel (SSD) (lbs/yd ³)	1795	1757	1719	1643
River Sand (SSD) (lbs/yd ³)	1197	1171	1146	1096
Target Air (SikaAir)	2.00%	3.50%	5.00%	8.00%

The rationale for only using one w/c of 0.50 is that the authors wanted to ensure all samples were properly consolidated and the selected w/c would help increase the dispersion of air bubbles within the concrete system, which will consequently help develop the new hardened air void characterization technique. The four different air contents were selected as they provided an even distribution of air void ranges for the investigation. Additionally, only two saw blade types and two polishing pad mediums were selected as they are the most common and recommended types/mediums for cutting and polishing hardened concrete samples in the United States. Similarly, the six polishing pad grit sizers were selected for the same reasons.

CHAPTER 3: FRESH AND COMPRESSIVE STRENGTH RESULTS

The results of the fresh and compressive strength testing of the concrete mixtures produced in this study can be seen in Table 3.1

Table 3.1 Fresh and Compressive Strength Results

Property	Control	Low Air	Medium Air	High Air
Fresh Density (lbs/ft ³)	146	144	143	139
Slump (in)	3.75	4.25	3.5	4.0
Measured Air Content (ASTM C231) (%)	2.1	3.7	4.9	8.3
Air Content (SAM) (%)	2.3	3.4	5.2	8.7
SAM Number	0.61	0.58	0.39	0.12
7-day compressive strength (psi)	5086	4557	4328	3890
28-day compressive strength (psi)	6719	5723	5340	4280

The results shown in Table 3.1 are all as expected based off the literature, experiences and the corresponding mixture proportions. The fresh density results decrease with an increase in air content, which is expected since the air has negligible weight and there is less concrete material in the system. The slump values were all within the target 3-5" range. The air values are also within the anticipated target range. Both the air content obtained from the ASTM C231 pressure method and the SAM meter appear to be in close alignment with each other. The SAM numbers decrease with an increase in air content, which is expected based off of the literature [27, 28]. A SAM number of 0.20 has been shown to correctly determine, over 90% of the time, whether the spacing factor is above or below the 0.008" limit [27, 28]. Therefore, an ideal SAM number is anything less than or equal to 0.20, which only the High Air mixture obtained. All other mixtures were above this value, which suggests the spacing factor is likely above the 0.008" spacing factor limit. The 7-day and 28-day compressive strength values were also as expected. All strengths showed a decrease in compressive strength with an increase in air content. The literature states that for every 1% increase in air content this causes a reduction in the compressive strength of about 500 psi [29].

CHAPTER 4: HARDENED CONCRETE SAMPLE PREPERATION

DISCUSSION AND RECOMMENDATIONS

This chapter is broken up into two major sections, Section 4.1 - the development and discussion of the preparation steps investigated, which includes information regarding why certain equipment, materials, and procedures were recommended, and lastly Section 4.2 - the recommended hardened concrete sample preparation steps necessary for hardened air void analysis using the new alternative method, as well as traditional methods outlined in ASTM C457 [11].

4.1 DEVELOPMENT AND DISCUSSION OF PREPERATION STEPS

4.1.1 Sample Cutting

Multiple 4" (dia.) x 8" (length) concrete cylinders were cast and prepared for hardened sample preparation. Therefore, all hardened samples were cut from 4" (dia.) x 8" (length) concrete cylinders. In the cutting process, a wet masonry saw from Humboldt Manufacturing was used, as seen in Figure 4.1.



Figure 4.1 Wet masonry saw from Humboldt.

Two different saw blades were investigated and are two current options for concrete saw blades; i) a 20" masonry saw blade seen in Figure 4.2a and ii) a 14" diamond cut-off wheel blade seen in Figure 4.2b.

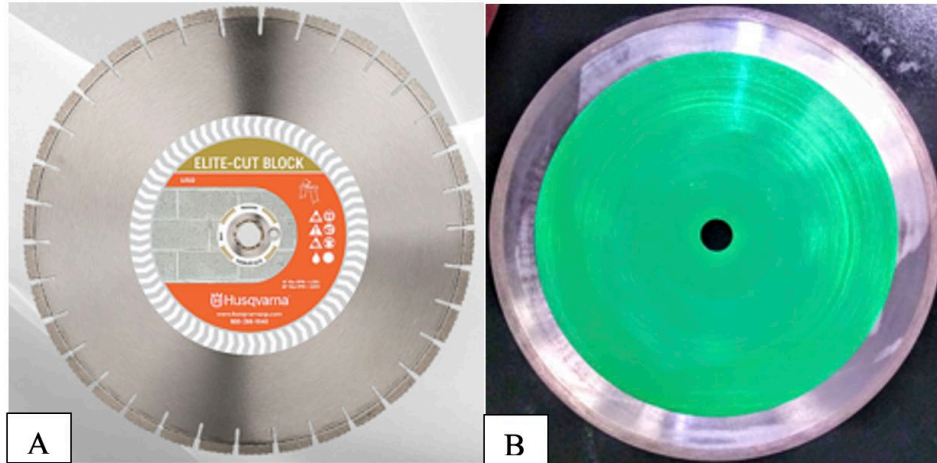


Figure 4.2 The two sawblades investigated in this study.

Two different blades were used in this study to determine the speed and cut quality of the different blades, and represent two current options for saw blades. The masonry saw blade is a common saw blade found in concrete materials labs, often purchased together with the wet saw. From experience, this blade tends to leave small grooving along the cut surface. A smoother cut from a saw blade, will ultimately result in less polishing time in the next steps, therefore an additional diamond saw blade was investigated. After an internet search, and discussions with equipment suppliers, it was discovered that the 14" diamond cut off blade, could produce superior cuts to the typical masonry saw blade. Both companies state that their blades can last for "thousands" of cuts, unfortunately the authors were unable to confirm or deny this claim. However, both blades showed no signs of wear after cutting all samples required (approximately 50 cuts were made) for this investigation. Currently, the masonry saw blade has a noticeably higher cost than the other. Due to project time and budget limitations, only two blades were investigated in this study.

When using either blade with the saw, a c-clamp was used to safely hold the sample flush against the edge of the rolling table portion of the wet saw, as seen in Figure 4.3. This helped to ensure that a straight cut was achieved.



Figure 4.3 Using a c-clamp to mount the concrete sample to the saw table.

The cylinders were cut parallel to the 4" diameter end of the cylinder into nominal 0.75" thick, circular, samples. The orientation and cut direction can be seen in Figure 4.3. On average one 8" long concrete cylinder would produce 6 – 7, 0.75" thick samples, as the cylinder became unsafe to mount or hold by hand for further cutting. On average, a single cut from the masonry saw blade took approximately five minutes. A two-minute cut could be achieved but the quality of the cut decreased. Even at a five-minute cut speed, the cut surface often exhibited small grooving from the blade along with a raised edge that was protruding from the cut surface. The raised edge is an issue as this edge will first need to be polished through before the majority of the sample will begin to be polished. The grooving was typically very fine and not as exaggerated as the raised edge. It could be seen with the naked eye and felt by hand. It was difficult to capture a photo of the grooving, but tended to show up better when the sample was wet in the reflected light. The cut quality of the masonry saw blade can be seen in Figure 4.4.

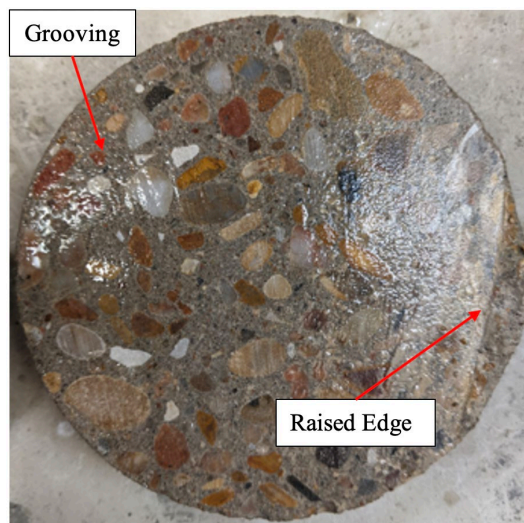


Figure 4.4 Masonry saw blade cut quality.

On average, a single cut using the diamond cut off blade would take approximately two minutes, which was the quickest and safest cut speed noted for this blade and saw configuration. It was observed that the cut quality with the diamond cut off blade was better than the masonry saw blade. There was little to no visible grooving left from the saw and the raised edge issue rarely occurred. An example of the cut quality from the diamond cut off blade can be seen in Figure 4.5.



Figure 4.5 Diamond cut off blade cut quality.

Based off of these observations, it was concluded that of the two saw blades investigated in this study, the diamond cut off blade is the more efficient blade to use for cutting hardened concrete samples for hardened air void analysis. The final saw cutting recommended procedures can be found in Section 4.2.2.

4.1.2 Sample Polishing

In this investigation a Struers Abramin auto-polisher was used, which can be seen in Figure 4.6.



Figure 4.6 Struers Abramin Auto-Polisher.

The Struers Abramin auto-polisher uses a 12" base that can rotate at either 150rpm or 300rpm clockwise. The polishing arm can apply a pneumatically applied force of 30N – 600N (6.7lbs – 134.8lbs). An aluminum fixture was constructed, in house, to fit in the polishing arm and to mount either a 4" diameter or 4" square concrete sample. The polishing arm rotates at 150rpm clockwise. The auto-polisher can automatically dispense water as a polishing lubricant. Once the desired force, base rotation speed, duration of polish, and rate of dispensed water is selected, the polisher can be engaged for the desired duration.

Based off the literature and discussions with manufacturers there are currently two popular mediums used to polish concrete samples, silicon carbide paper polishing discs and diamond metal backed polishing discs. Silicon carbide paper polishing discs are typically sold in packs of 100 and cost up to \$300 per 100pack of polishing discs depending on the grit size. These types of polishing discs typically have an adhesive backing, and need to be applied to an accompanying metal support disc. The base of the Struers Abramin auto-polisher is magnetic (as well as many other auto-polishers) and the support disc will magnetically attach to the base of the auto-polisher. However, once the silicon carbide polishing disc is spent, it will need to be removed from the metal support disc and a new one applied. The diamond metal backed polishing discs are sold individually and cost upwards to \$600/disc. However, these diamond polishing discs are pre-adhered to a metal backing, therefore do not require a metal support disc to attach to the polisher.

In this investigation, it was discovered that the first polishing step, using the coarsest polishing medium, is the most crucial in producing a suitable surface for further analysis. In this first polishing step, it is necessary to produce a completely flat polish that removes all grooving and other uneven surfaces created from the saw cutting. Using the diamond cut off blade discussed in the previous section drastically reduced the time required to achieve a completely flat polish from the first polishing step. The procedure developed to achieve a completely flat polished surface is discussed in Section 3.4.

It was observed that, when completing the first polishing step, using the silicon carbide polishing discs at grade 80 would require on average 2-3 polishing discs to achieve a completely flat surface. This was completed at a recommended applied force range of 150N-300N (33.7lbs – 67.5lbs). This was also a laborious process because the polishing disc had to be periodically checked to see if it had worn through. It was possible to see that the polishing discs was beginning to wear, as one side of the polishing disc is visible while polishing, but it was difficult to make an accurate interpretation while the polishing disc was spinning and wet. Therefore, the auto-polisher had to be completely stopped, the polishing disc removed, dried with a forced air hose, and then a decision to replace was made. If it was time to replace the silicon carbide polishing paper, it had to be removed from the metal support disc and a new one adhered.

Removing the polishing paper from the metal support disc was completed with the aid of a handheld paint scrapper tool, a razor blade scraper, and rubbing alcohol for any residue. This process could be sped up with an additional metal support disc pre-loaded with a new silicon carbide polishing disc and swapped when needed.

In addition to checking the polishing paper, the concrete sample needed to be checked, to determine if a completely flat polish was achieved (specifics regarding this process are detailed in Section 3.4). It was difficult to settle on a specific amount of time to stop the polisher and check the polishing paper and concrete sample, as the degree of polishing required per sample varied. The polishing time can also vary on the force applied, the rpm of the polishing pads, and more specifically, the sample hardness, paste amount, and aggregates used in the concrete. On average, with the samples produced in this study, a silicon carbide polishing disc would begin to wear out between 20-30 minutes at 300N (67.5lbs) force at a platen speed of 300rpm. As previously stated, 2-3 Silicon Carbide polishing discs were required to achieve a completely flat polish, therefore, at minimum the first polish could be set for 20 minutes without stopping to save time. Once the sample was observed to be nearly complete, the polishing time periods were set to 2-5 minutes depending on how close the sample was to complete. Following each short duration, the sample was checked. This procedure was followed in order to preserve the life of the polishing discs, as a limited amount were available for this study due to budget limitations. This process was more involved and required more operator time, however, if one had unlimited silicon carbide polishing discs, the polisher could simply be set to 30 minutes at 300N (67.5lbs) for three new polishing discs, and on average the sample would be completely flat following this polishing regimen.

It was observed that the diamond polishing discs were less labor intensive and had a much longer life than the silicon carbide counterparts. Since the diamond discs are pre-metal backed, the polishing paper does not have to be removed or adhered to a support disc, so that process is completely removed with these polishing discs. Additionally, these polishing discs last much longer. At the time of this writing approximately 50 surfaces have been polished, and there is no sign of wear on any of the discs. According to the manufacturer, hundreds of samples can be polished per disc. It was also noticed that, it took on average 20 minutes to polish a sample completely flat with the coarsest diamond polishing disc (260 μ m) at 300N (67.5lbs) force at a platen speed of 300rpm. Due to the robust nature of the diamond polishing discs, higher forces were investigated in attempt to reduce the polishing time. The optimum configuration to reduce the polish time was 500N (112lb) at a platen speed of 300rpm with water as the lubrication. This configuration would produce a completely flat surface at an average polishing time of 10 minutes. Based off these observations, it was concluded that the diamond metal backed polishing discs were worth the higher cost in this study. The final polishing recommended procedures can be found in Section 4.2.4.

4.1.3 Contrast Enhancement of Hardened Concrete Samples

The contrast enhancement process is necessary for further hardened air void analysis using the new alternative digital optical microscope method. It is possible to use the microscope on the non-contrast enhanced samples, however, the on-board counting and measuring software will not be able to distinguish between all of the features on the surface of the sample. Therefore, it is necessary to enhance the contrast between the air voids and the remaining portion of the sample. The final recommended contrast enhancement steps can be found in Section 4.2.6.

4.1.3.1 Blackening of Sample

Two different blackening methods were attempted in this investigation i) using a black permanent marker, and ii) using water-soluble acrylic ink and roller.

4.1.3.2 Black Permanent Marker

Previous studies [2-8] have developed a hardened concrete air void analysis technique using a flatbed scanner. In these studies, the procedures also require the samples to be contrast enhanced, and the samples to first be blackened out. The majority of these authors suggest simply using a black permanent marker, such as a chisel tip Sharpie brand marker. These studies also specify that the ink should be applied in a line-by-line, left-to-right, application in which each sequential line is overlapped with the previous line. After the sample is completely blackened from top-to-bottom with this method, the authors state to apply one additional layer perpendicular to the previously applied layer, to ensure the sample is sufficiently blackened. It is understood that this method applies the minimum amount of ink necessary to blacken the surface, and not interfere with the following preparation step. The following preparation step requires the addition of a fine white powder (discussed in further detail in section 2.3.2). Adding too much ink, or adding it in a quick, random pattern would result in ink bleeding into the white powder (once it is applied), coloring it a purple/gray color, no matter how long the ink was left to dry.

Additionally, coloring the surface in a quick, random, pattern could unintentionally fill the small air voids with ink. It was also discovered that when using a Sharpie brand black chisel tip permanent marker, the ink would not apply evenly, leaving a streaky application. This was true even with a brand-new marker. It was possible that the sample surface was not providing enough friction between the tip to draw ink in an even manner. It was found that a Staples brand black chisel tip permanent marker rarely left a streaky finish. However, it was important to note that both markers did not leave a completely flat black finish, in that the individual lines could still be seen with the naked eye in the light reflection, even with a thorough non-streaky application. This was especially the case, if upon initial application, the marker did not apply evenly, or if the operator accidentally did not overlap the lines properly, and required correction. This finish quality could also be described as a non-homogenous blackening of the surface, as the individual lines (although black) could be individually identified in the light. This finish quality could be an issue when analyzing the sample under a microscope as they may reduce accuracy due to differences in light reflections.

4.1.3.3 Water-Soluble acrylic Ink and Roller

Fonseca *et al.* [30] reported that black permanent markers often contain a resin, leaving the surface sticky. This was noticed with both the Sharpie and Staples brand permanent markers discussed in Section 4.2.6. The stickiness is potentially an issue, as the white powder application in the next step could stick to the surface. Therefore, Fonseca *et al.* [30] suggested using a water-soluble acrylic ink and roller. This type of ink does not contain a resin, so it should not leave a sticky surface. The authors of this report found the use of the water-soluble acrylic ink to be the superior blackening method to the permanent marker. Although, it is slightly more expansive than the markers, this method produce a surface that appeared

much blacker than the markers, it was not sticky, and it applied evenly (no striations as with the markers). As discussed more thoroughly in Section 4.2.6, the last step in the contrast enhancement procedure is to use mineral oil to remove white powder stuck to the surface. With the black marker method, the mineral oil simply removes the fine particle from view, by making them less reflective, and when the sample dries, they come back into view. However, with the ink and roller method, the oil physically removes the fine particles from the surface, since the surface is not sticky, therefore no re-application is needed if the samples are to be analyzed at a later date. Therefore, it is recommended that the blackening of the sample surface be completed with a black water-soluble acrylic ink and roller.

4.1.3.4 White Powder

In order to enhance the contrast between the air voids and the rest of the sample a white powder is required to fill the air voids. ASTM C457 [11] Procedure C currently says to use a white powder, and offers barium sulfate, wollastonite, or titanium dioxide with a median particle size of 2-3 μm as some suggestions. However, the standard does not provide any further detail on these white powders. Other literature [30] has also suggested using a zinc oxide paste for this step. Zinc oxide is typically found to be the primary ingredient in sunscreen and diaper rash/skin cream. Irrespective of the brand, these pastes typically list 20% zinc oxide as their only ingredient.

Therefore, an over-the-counter diaper rash cream with 20% zinc oxide was initially used for this step, due to it being readily available and cheap. However, the zinc oxide paste caused many problems, the primary being that it tended to dissolve the ink from the surface resulting in the paste becoming a purple/gray color. Therefore, an over-the-counter diaper rash cream with zinc oxide was deemed unusable for this step. Fonseca *et al.* [30] investigated multiple white powders for the same purpose of enhancing the contrast of air voids in a blacked out concrete sample. The authors investigated the following white powders; Barium Sulfate with a mean particle size of 3 μm , titanium dioxide with a mean particle size of 0.5 μm , silicon oxide with a mean particle size of 2 μm , and corn starch with a mean particle size of 9 μm . Fonseca *et al.* [30] found that the titanium dioxide particles were too small and filled in the very small imperfections that remained from polishing. In contrast, the corn starch showed to be too coarse. An individual corn starch particle would fall into an air void and “bridge” itself from edge-to-edge of the air void resulting in parts of the air void unfilled. This will result in an underestimation of the air void content when the sample is analyzed. Both the silicon oxide and barium sulfate powders were deemed to be an ideal particle mean size; small enough to properly fill all air voids, but not too small to fill in the very small defects.

Barium sulfate powder was ultimately recommended over the silicon oxide powder as it was much whiter and will provide a better contrast between the sample. The authors did not investigate wollastonite; however, it was difficult to find wollastonite to purchase that contained a mean particle size of 2-3 μm . However, barium sulfate with a 3 μm mean particle size was found to be readily available. Based off these findings and recommendations, a barium sulfate powder with a mean particle size of 3 μm was acquired and used on the polished concrete samples.

4.1.3.5 Correcting the Black Surfaces

Following the compaction (procedures discussed in Appendix A.1) of the barium sulfate powder, it was observed that small cracks in the aggregates and even air voids in the aggregates will be highlighted by the white powder. These need to be removed, as they will contribute to the air void analysis and invalidate the results. To remove these features, a black permanent marker can be used to black-out these features. These small corrections do not leave any striations as observed when using the black permanent marker to completely blacken the surface. Additionally, a handheld magnifying lens can also be used to assist with this step.

4.1.3.6 Mineral Oil

It was observed that very small amounts of compacted barium sulfate powder remain after its removal from the surface. The small amounts of powders are not embedded in an air void or an aggregate feature, but are simply stuck to the surface. It was found that the best way to remove these small amounts of powder is to apply mineral oil to the surface. Regarding the blacked-out surface with the permanent marker, this process does not technically remove the powder from the surface, but they are removed from view in regards to further analysis, such that the particles are small enough to absorb the mineral oil and become non-reflective. This is pertinent to know, as the mineral oil will eventually dry and the small amounts of Barium Sulfate powder will become visible again. The drying process takes approximately 10-15 minutes in a laboratory setting at room temperature. Therefore, it is necessary to consider when further analysis will take place, as this step should take place immediately before future analysis. It is noted that, mineral oil can be re-applied multiple times and it does not affect the analysis. However, as previously mentioned, the authors of this report recommend using a black water-soluble acrylic ink to blacken the surface, and it was observed that the mineral oil does remove the Barium Sulfate from the surface of the ink-processed samples, and in most instances, the mineral oil does not need to be applied again.

CHAPTER 5: ASTM C457 SAMPLE CHARACTERIZATION

5.1 METHODOLOGY

Following the sample production and preparation of the hardened concrete samples, the samples, were analyzed in accordance to ASTM C457-16 Procedure A (linear traverse method) and Procedure B (modified point and count method). The contrast enhanced procedures described in Appendix A.1 meet the sample preparation requirements of ASTM C457 Procedure C (contrast enhanced method). ASTM C457 states that both Procedure A and B can be performed on a contrast enhanced sample if additional petrographic data is not required and additional information can be determined from the mix design [11]. Additionally, completing Procedure A and Procedure B on the contrast enhanced samples will provide better correlation to the future alternative air void characterization method, which will also be completed on the same contrast enhanced samples.

The hardened air void analysis was first completed using a Linear Traverse Machine connected to a computer for data processing, which meets the requirements of ASTM C457. Although the system is called a Linear Traverse Machine, the provided software is geared towards completing a modified point and count procedure (Procedure B), in that the stage moves and stops at pre-determined points and information is recorded based on what is observed at each point. Despite this, a linear traverse procedure (Procedure A) can also be completed using the Humboldt Linear Traverse Machine, however, the data has to be collected, managed, and calculated with an electronic spreadsheet (or other data management software), in combination with the linear traverse software. The Linear Traverse Machine hardware set-up can be seen in Figure 5.1.



Figure 5.1 Linear Traverse Machine.

5.2 ASTM C457 RESULTS

In order to ascertain the quality of each polishing level discussed in Chapter 4 and Appendices A.1 and A.2, Procedure A and B was completed on samples polished using 260 μm , 125 μm , 70 μm , 30 μm , 15 μm , and 6 μm diamond polish discs. Additionally, each sample was analyzed a total of three times each. Since the samples produced in this study are circular, there could be variability in the assessment in regards to where the analysis begins relative to the sample. Both procedures require the starting point of a circular sample to be near the top and at one end of the initial traverse. However, slightly different results would be obtained if that starting point were different.

To control this, and to provide average results for each sample, a mark was placed on the side of the sample, and for the first assessment the mark was pointing in the north direction in regards to the traverse stage. ASTM C457-16 Note 8 describes the “East-West (E-W)” direction as the direction from the operator’s left to right, and “North-South (N-S)” refers to the direction perpendicular to E-W, that is, the directions are analogous to those on a map. Therefore, Procedure A and B were completed on one sample in which the mark was oriented towards the north direction. Then the sample was rotated 45° to the east, such that the mark was oriented towards the north-east direction, then Procedure A and B were completed. Lastly, the mark was rotated an addition 45° to the east, such that the mark was oriented towards the east direction, and Procedure A and B were completed one last time on the same sample. The three data points for each polished surface were then averaged and reported in Table 5.1 and graphically presented in Figures 5.2 – 5.5.

Table 5.1 ASTM C457 Procedure A and B Results.

Control - ASTM C231 Measured Air Content = 1.8%, SAM No. = 0.65							
Procedure A							
Polish Pad Grit Size	260µm	125µm	70µm	30µm	15µm	6µm	AVG
Air Void Content, %	2.1	2.2	1.9	2.1	2.2	2.0	2.1
Spacing Factor, in	0.0191	0.0203	0.0193	0.0221	0.0193	0.0212	0.0202
Specific Surface, in ² /in ³	422	472	459	430	410	430	437
Procedure B							
Polish Pad Grit Size	260µm	125µm	70µm	30µm	15µm	6µm	AVG
Air Void Content, %	1.7	1.6	1.6	2.0	1.7	1.7	1.7
Spacing Factor, in	0.0212	0.0195	0.0218	0.0158	0.0210	0.0183	0.0196
Specific Surface, in ² /in ³	437	420	451	411	431	419	428
Low Air - ASTM C231 Measured Air Content = 3.5%, SAM No. = 0.59							
Procedure A							
Polish Pad Grit Size	260µm	125µm	70µm	30µm	15µm	6µm	AVG
Air Void Content, %	3.7	3.5	3.7	3.8	3.6	3.7	3.7
Spacing Factor, in	0.0128	0.0131	0.0140	0.0155	0.0133	0.0120	0.0135
Specific Surface, in ² /in ³	591	599	585	572	583	573	584
Procedure B							
Polish Pad Grit Size	260µm	125µm	70µm	30µm	15µm	6µm	AVG
Air Void Content, %	3.4	3.3	3.3	3.3	3.2	3.4	3.3
Spacing Factor, in	0.0134	0.0148	0.0140	0.0151	0.0153	0.0132	0.0143
Specific Surface, in ² /in ³	572	582	581	573	582	571	577
Medium Air - ASTM C231 Measured Air Content = 4.8%, SAM No. = 0.39							
Procedure A							
Polish Pad Grit Size	260µm	125µm	70µm	30µm	15µm	6µm	AVG
Air Void Content, %	5.1	5.0	5.2	5.1	5.2	5.0	5.1
Spacing Factor, in	0.0096	0.0092	0.0098	0.0094	0.0098	0.0093	0.0095
Specific Surface, in ² /in ³	627	632	624	639	641	619	630
Procedure B							
Polish Pad Grit Size	260µm	125µm	70µm	30µm	15µm	6µm	AVG
Air Void Content, %	4.2	4.3	4.3	4.1	4.2	4.3	4.2
Spacing Factor, in	0.0110	0.0112	0.0109	0.0115	0.0107	0.0102	0.0109
Specific Surface, in ² /in ³	598	605	613	594	610	611	605
High Air - ASTM C231 Measured Air Content = 8.7%, SAM No. = 0.12							
Procedure A							
Polish Pad Grit Size	260µm	125µm	70µm	30µm	15µm	6µm	AVG
Air Void Content, %	8.5	8.2	8.3	8.4	8.4	8.5	8.4
Spacing Factor, in	0.0072	0.0074	0.0075	0.0071	0.0073	0.0079	0.0074
Specific Surface, in ² /in ³	723	711	722	709	728	735	721
Procedure B							
Polish Pad Grit Size	260µm	125µm	70µm	30µm	15µm	6µm	AVG
Air Void Content, %	8.9	8.9	8.9	9.1	8.5	9.0	8.9
Spacing Factor, in	0.0069	0.0071	0.0073	0.0068	0.0069	0.0064	0.0069
Specific Surface, in ² /in ³	769	772	775	789	742	782	772

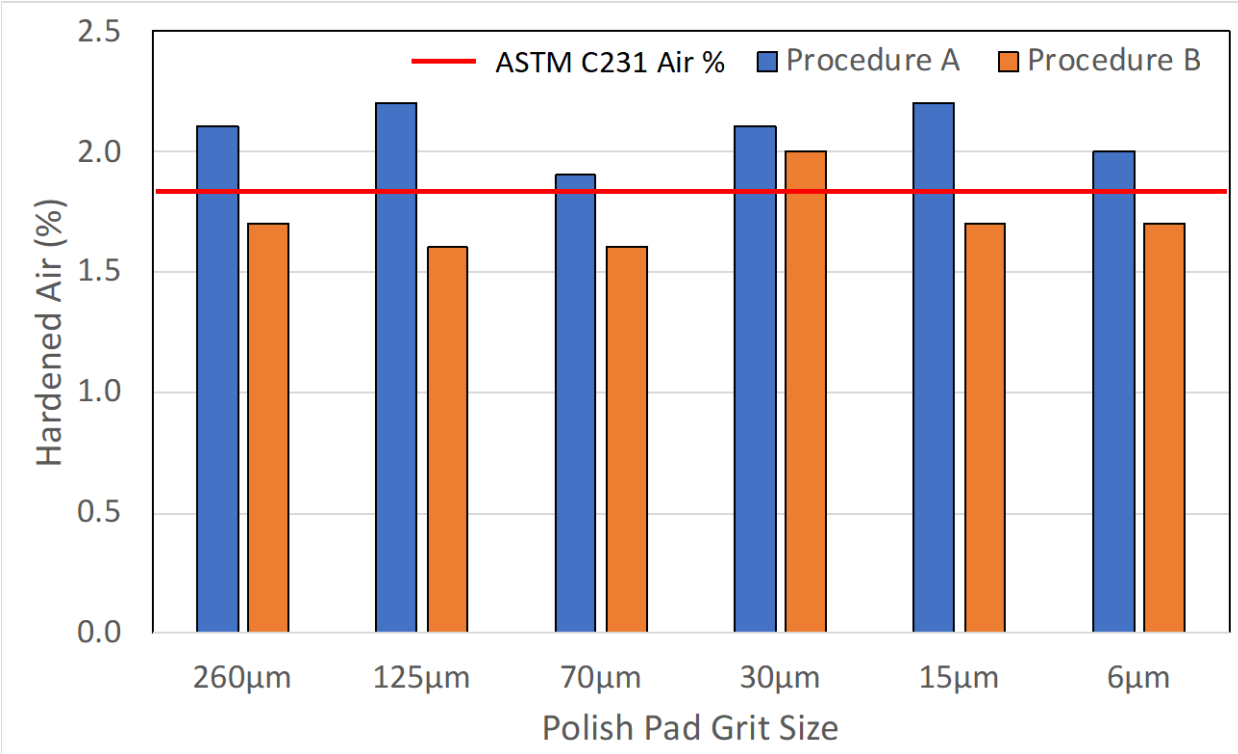


Figure 5.2 Control (2% Target) Hardened Air Void Comparison.

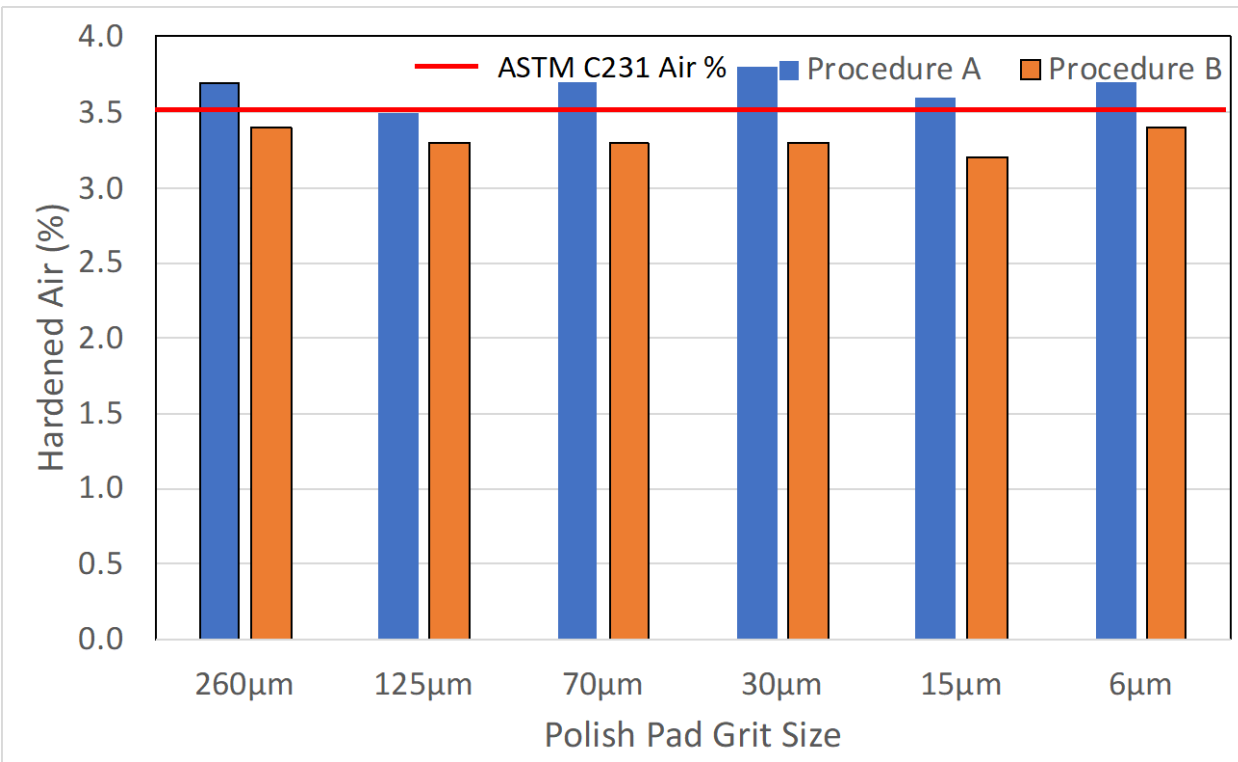


Figure 5.3 Low Air (3-5% Target) Hardened Air Void Comparison.

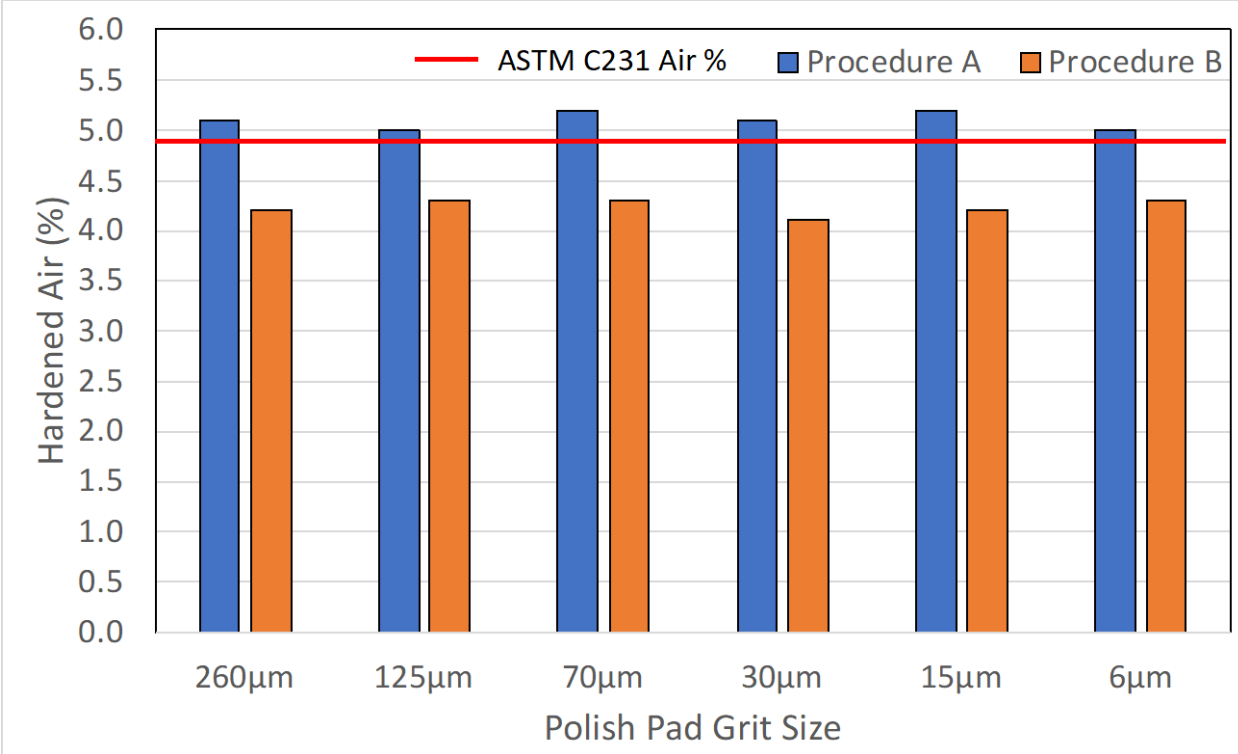


Figure 5.4 Medium Air (5-7% Target) Hardened Air Void Comparison.

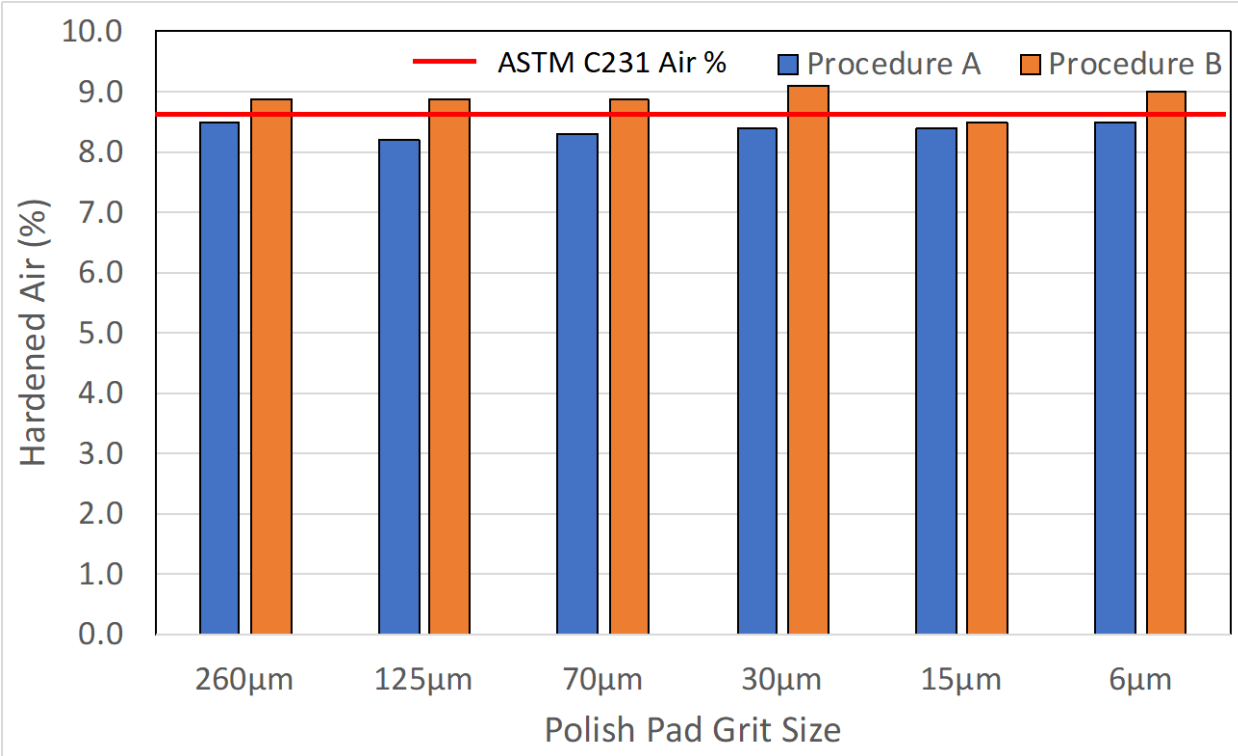


Figure 5.5 High Air (>8% Target) Hardened Air Void Comparison.

As seen in Table 1 and Figures 5.2 – 5.5, both procedures produced hardened air void percentages similar to the fresh air content measured via ASTM C231. Observing the hardened air void values across each polish pad grit size reveals no significant change between subsequent smaller grit sizes. The average percent difference across each polish pad grit size was 3.8% with a range of 1.4 – 7.9%. This amounted to an average hardened air void difference of only 0.1 across all samples. Comparing the average hardened air void percentage across all polish pad grit sizes to that of the ASTM C231 fresh air percentage, reveals an average percent difference of 6.7% with a range of 2.1 – 14.6%. These fresh versus hardened air void percentage differences are also consistent with the reported values in the literature [13,27,33,34].

It is also observed that, on average, Procedure A produced results that were slightly higher than the ASTM C231 results, and Procedure B produced results that were, on average, below that of ASTM C231 results. This result is reversed with the high air samples. This is believed to be due to the nature of the testing, in which with Procedure B, the pre-determined stops are established and stops can miss an air void and/or be on the edge of an air void, and it is up to the operator's opinion whether to count the stop in an air void or not. For consistency purposes, the same operator completed all of the analysis, such that the decision was subject to the same individual. According to Hover (2006) [1], this decision process can have a higher effect on the measured air void percentage with specimens that contain lower air percentages, as the air voids could be smaller and/or more spaced out. This provides further insight as to why the Procedure B values were consistently lower than Procedure A values, aside from the high air samples.

In regards to the spacing factor and specific surface values, they also did not show any significant difference between the different polish pad grit sizes. The results for both are also as expected, and in the appropriate range and agree with the literature [13,27,33,34]. When comparing between the two procedures, an average percent difference of 7.5% with a range of 3.1 – 13.7% was observed for the spacing factor, and an average percent difference of 3.5% with a range of 1.2 – 6.7% was observed for the specific surface values. Also, the spacing factor values are consistent with the measured SAM numbers, such that a SAM number of 0.20 or less typically produces a spacing factor of 0.008" or less. As seen in Table 3.1 the control, low air, and medium air mixtures all obtained a SAM number above 0.20, and all of those mixtures recorded a measured spacing factor of above 0.008". Whereas the high air mixture produced a SAM number of 0.12 and recorded an average spacing factor of 0.0069". As indicated by Ley *et al.* (2013) [34] this is typically the case 90% of the time and was the case with the measured samples in this study.

Overall, the results of the ASTM C457 characterization were as expected and in an appropriate range. Additionally, the results indicate that for the samples tested, it is not necessary to polish any lower than 260 μ m, as long as the 260 μ m was polished sufficiently as outlined in Chapter 4/Appendices A.1 and A.2. This result indicates that time can be saved on the sample preparation step as well as cost, as the subsequent polish pads do not need to be purchased. It should be noted that, the samples produced and polished in this study did not exhibit any air void degradation or elongation from the polishing process, and thus required no paste strengthening with lacquer or by other means as described in ASTM C457 [11] or by other authors [27,34]. This could be the factor that allowed for the subsequent polishing with finer grits to be insignificant, as the authors did not investigate the impact of paste strengthening. Additionally, all samples polished in this study had a minimum cured age of 28-days, which will lead to a stronger paste.

It is likely that paste strengthening is required for younger samples. Additionally, Hover (2006) [1] indicates that faulty or incomplete specimen preparation can be a source of hardened air void characterization error. Therefore, care should be taken to observe the quality of each subsequent polish step with a microscope or handheld magnifying glass as discussed in Chapter 4.

CHAPTER 6: ALTERNATIVE AIR VOID CHARACTERIZATION METHOD TESTING AND DEVELOPMENT

6.1 INTRODUCTION TO THE ALTERNATIVE METHOD

This chapter is broken up into three major sections, Section 6.2 - a discussion of the newly developed digital optical microscope method, Section 6.3 – how to calculate the key hardened air void information and results, and Section 6.4 – the recommended equipment and procedures to produce a hardened air void analysis.

6.2 ALTERNATIVE DIGITAL OPTICAL MICROSCOPE METHOD

6.2.1 Hardware

For this study a Keyence – VHX 7000 series was used, which is the most current available microscope sold by Keyence. The Keyence – VHX 7000 digital optical microscope can be seen in Figure 6.1.

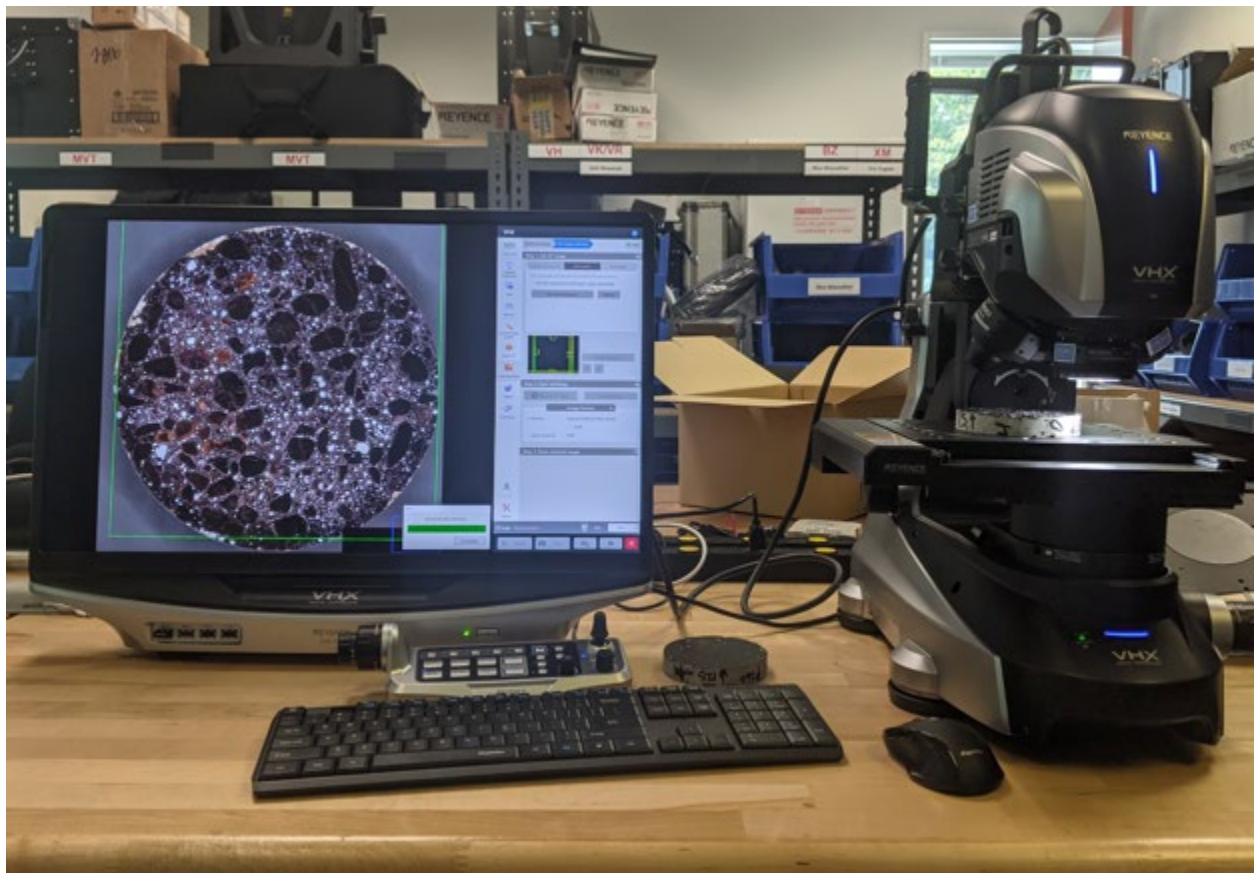


Figure 6.1 Keyence – VHX 7000 Series Digital Optical Microscope.

As seen in Figure 6.1, the Keyence digital optical microscope system consists of a monitor/computer unit, the microscope unit (automated stage, optical lenses, and various lighting), and peripherals (controller unit, keyboard, and mouse). The 7000 series is the 5th generation of the Keyence microscopes and delivers measurements with ultra-high accuracy in 4K resolution. The microscope unit can deliver magnifications in the range of 20x – 6000x. This is done automatically, without the need of switching objective lenses or other parts. The stage, where the sample rest, is also completely motorized and automatic. The stage has a movement range of 4-inches (100 mm) in both the X and Y horizontal directions, which can easily be manipulated by a mouse click or using the controller unit. The controller unit is also very intuitive, and can control many functions including, focus, magnification, stage orientation, lighting, and more.

6.2.2 Software Capabilities

The Keyence – VHX 7000 series system comes with on board stitching, counting, and measuring software, which are key for the hardened air void analysis. The stitching feature, is the critical step that will save time in the characterization process. As with any microscope, the ASTM C457 recommended 50x magnification will not show the entire sample within the magnified image, and any assessment has to be completed incrementally as the sample is re-positioned below the lens. However, the stitching feature on the Keyence – VHX 7000 will automatically move, capture, and stitch all areas within the bounds established by the operator. The Keyence stage offers enough actuation, such that an entire 4-in. diameter (or 4-in. x 4-in. square) [100mm. in diameter (or 100mm x 100mm square)] concrete sample can be completely stitched in one stitching operation. This allows the entire sample to be characterized in one complete assessment and the user to view the entire sample in one singular image.

It should be noted that the stitching software is sophisticated enough that it is not simply placing images next to each other, in which there could be an overlap in the analysis, but it is actually pixel matching hundreds of thousands of pixels across each image, such that it is, in fact, producing one complete image. On a 4-in. (100mm) diameter concrete sample, at a 50x magnification, the entirely automated stitching process can be completed in approximately 10 minutes. Following the stitching, the Keyence microscope system has the ability to automatically count and measure any feature desired on the sample. However, the counting and measuring software is more efficient and accurate when the particular area of interest has a different contrast from the background. This is why contrast enhancing the samples is required, as the software will easily pick up all of the white voids from the black background.

The counting and measuring process is completed automatically once the user sets the boundary of the desired assessment area. Therefore, the operator can count and measure specific areas or the entire area if they desire. For each specimen in this study virtually the entire sample was analyzed by drawing a circle around the entire sample to set the bounds of the assessment area. A slightly smaller circle was used as the very edge of certain samples contained edge defects, that would interfere with the analysis, and thus were removed from the assessment. The size of the smaller circle used for the assessment area had an approximate diameter of 3.9-in (99mm). The user can establish this same circle be used for future analysis to maintain consistency across other analysis. This was done for the analysis completed in this study for consistent comparison. A fully stitched and measured sample can be seen in Figure 6.2.

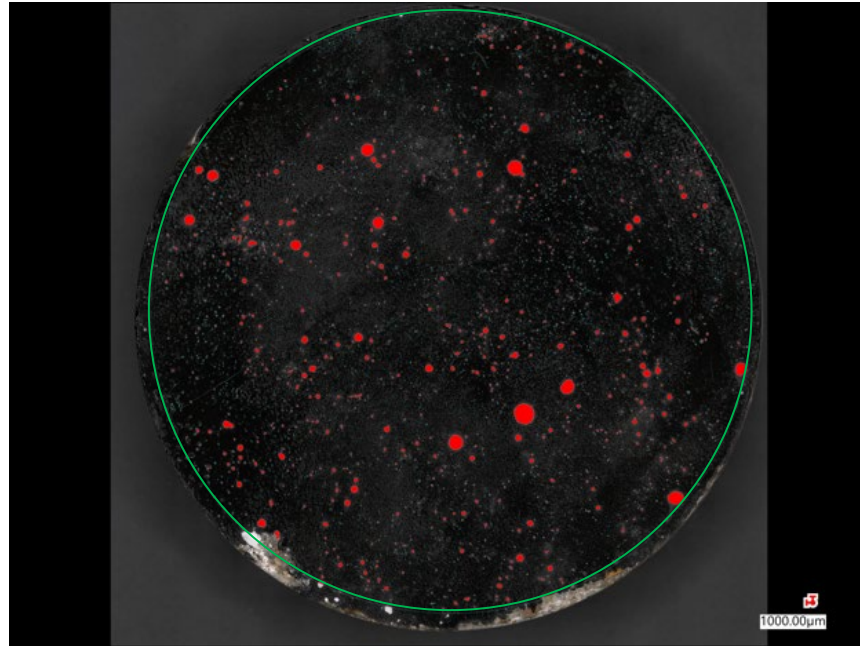


Figure 6.2 Stitched and Measured Sample.

In Figure 6.2, a contrast enhanced and polished sample from Chapter 4 can be seen, which was fully stitched and the voids have been counted and measured. This image simply shows the sample itself, the boundary line, which was input by the operator, and the air voids that have been counted. For clarity purposes a brighter green circle has been drawn on the screenshot such that the boundary line is more visible in Figure 6.2. First, the boundary can be observed as the teal circle that is just inside of the edge of the sample. As previously stated, this can be established by the operator as any desired shape. A circle was chosen as it removes very little of the sample, while also ignoring the edges of the sample that are chipped from the saw cutting. Excluding these parts ensures that objects in those areas are not counted in the counting and measuring process. The next thing to observe are the highlighted areas in red, which also have a teal outline. These are the objects/air voids that have been counted and measured. Additionally, small teal-colored dots can be seen throughout the sample. Those are also objects/air voids, but are so small that the red color is not visible at this magnification, but only the teal outline is visible, making them appear as only teal-colored dots. These colors can also be changed by the operator, and the current color scheme is the default and was visible amongst the black and white of the sample.

Once the sample has been automatically counted in this manner, the user can investigate the sample at any magnification level to either select air voids that were not previously counted or deselect air voids, in which the operator feels were not in fact air voids, such as a defect, crack, or aggregate pop out. For example, in the bottom left-hand corner of the sample shown in Figure 6.2, there is a small white area that is connected to the chipped off area. This white area is filled with the Barium Sulfate powder, and within the bounds of the counting and measuring area, however, it is clear that it is not an air void (entrapped or entrained) due to its irregular shape (non-spherical) and was part of the chipped off area. Therefore, it was removed from the analysis. Additionally, some air voids that are present outside of the counting and measuring bounds can be added in. For example, on the very bottom of the sample in Figure 6.2, there are a few white, spherical, areas that were not counted due to them being outside of the counting and measuring boundary. For the purposes of demonstration, these were initially left

uncounted, but after the automatic counting has taken place, the operator can select these air voids to include them in the analysis. An additional feature of the counting and measuring software is that before the analysis takes place, the operator can input specific parameters, such as a minimum, maximum, or defined range of objects to count. Hover (2006) [1] described that the minimum entrained air void size ranges from 0.010–0.020 mm (0.0004–0.0008 in.) up to a maximum size of approximately 1mm (0.039 in.). Entrapped air voids from improper consolidation are typically larger than 1mm (0.039 in.) and have irregular shapes [1]. This information can be incorporated into the analysis to distinguish between entrained and entrapped air voids. Another feature of the analysis is regarding the circularity of the counted objects. The analysis measures the maximum horizontal distance and maximum vertical distance of a measured object and compares them to obtain the circularity. A circularity value of 1.00 indicates a perfect circle, as both values are the exact same. Therefore, an additional constraint the operator can input is a circularity range, such that the analysis is not counting objects that would not be considered an air void. Following the analysis, the software can produce a window in which all of the individual objects (air voids) are shown along with their individual area, as shown in Figure 6.3.



Figure 6.3 Individual Air Void Analysis Display.

Shown in Figure 6.3 is a window with all of the air voids that were counted and measured in this analysis; only a portion is shown in Figure 6.3, but the operator can scroll the window down to see the remaining air voids. In Figure 6.3, the window is set to display the air voids from largest to the smallest. From this window, the operator can select an air void from the window (as shown) and the specific air void on the sample will be highlighted (shown in purple on the right-hand side of the figure). Also observed in Figure 6.3, is an object that was removed from the analysis, which is not highlighted in red, and appears white in color (the original color) in the upper left-hand corner of the figure. Due to the shape of this object, it is likely a defect, an entrapped air void, which tend to be irregular in shape, or not an air void at all, which

is why it was removed. This process can also be completed faster by either entering a circularity constraint as discussed previously, or assessing the window shown in Figure 6.3, such that all objects/air voids are highlighted and can be removed quickly and easily. It is important to note that no circularity constraint was used in the analysis shown in Figure 6.3 for demonstration purposes. However, this method can still be used to quickly assess the measured air voids as a quality assurance procedure. In addition to the individual object images, an additional display window can be shown with measurement information about each object. An example of this can be seen in Figure 6.4.

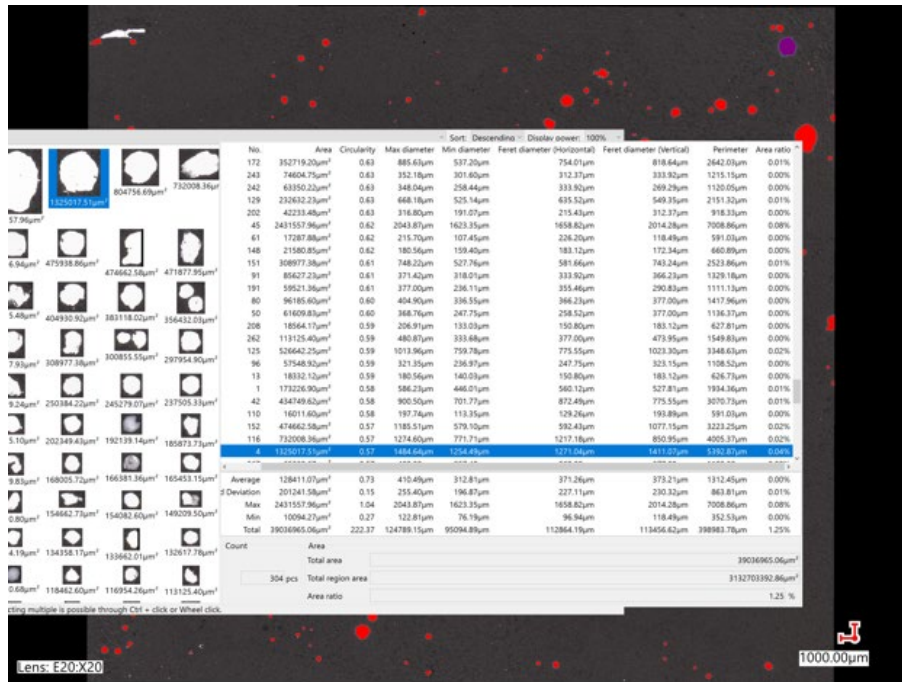


Figure 6.4 Object Measurement Information.

The display window with the measurement information can be exported to a .csv file and further analyzed using an electronic spreadsheet program. The measurement information shown in the screen shot in Figure 6.4 is difficult to see, therefore, an example .csv was created and a screen shot of that information can be better seen in Figure 6.5.

	B	C	D	E	F	G	H	I	J	K	L	M	N
65													
66	Measurement result												
67	Title	Auto area measurement results data											
68	Date saved	7/21/21 11:30 AM											
69	Comment												
70	[Statistics]												
71		Area	Unit	Circularity	Unit	Max diameter	Unit	Min diamet	Unit	Feret diam	Unit	Feret diam	Unit
72	Average	8654.19	µm ²	2.27		51.08	µm	25.27	µm	61.01	µm	61.27	µm
73	Standard Deviat	108999.38	µm ²	2.03		116.58	µm	82.5	µm	99.98	µm	101.09	µm
74	Max	10866499.11	µm ²	6.28		5084.44	µm	2904.63	µm	3188.67	µm	5014.07	µm
75	Min	533.9	µm ²	0.14		0	µm	0	µm	23.11	µm	23.11	µm
76	Total	145814397.8	µm ²	38268.17		860696.56	µm	425737	µm	1027884	µm	1032390	µm
77	[Main]												
78	No.	Area	Unit	Circularity	Unit	Max diameter	Unit	Min diamet	Unit	Feret diam	Unit	Feret diam	Unit
79	1	533.9	µm ²	1		0	µm	0	µm	23.11	µm	23.11	µm
80	2	1067.8	µm ²	6.28		23.11	µm	0	µm	46.21	µm	23.11	µm
81	3	533.9	µm ²	1		0	µm	0	µm	23.11	µm	23.11	µm
82	4	48051.14	µm ²	0.92		292.27	µm	184.85	µm	207.96	µm	300.38	µm
83	5	533.9	µm ²	1		0	µm	0	µm	23.11	µm	23.11	µm
84	6	533.9	µm ²	1		0	µm	0	µm	23.11	µm	23.11	µm
85	7	1067.8	µm ²	6.28		23.11	µm	0	µm	23.11	µm	46.21	µm
86	8	3737.31	µm ²	1.13		83.31	µm	29.24	µm	69.32	µm	92.43	µm
87	9	3203.41	µm ²	1.93		51.67	µm	32.68	µm	69.32	µm	69.32	µm
88	10	1067.8	µm ²	6.28		23.11	µm	0	µm	46.21	µm	23.11	µm
89	11	1067.8	µm ²	6.28		23.11	µm	0	µm	23.11	µm	46.21	µm
90	12	533.9	µm ²	1		0	µm	0	µm	23.11	µm	23.11	µm
91	13	1601.7	µm ²	3.23		32.68	µm	16.34	µm	46.21	µm	46.21	µm
92	14	1067.8	µm ²	6.28		23.11	µm	0	µm	46.21	µm	23.11	µm
93	15	1601.7	µm ²	3.23		32.68	µm	16.34	µm	46.21	µm	46.21	µm
94	16	533.9	µm ²	1		0	µm	0	µm	23.11	µm	23.11	µm
95	17	533.9	µm ²	1		0	µm	0	µm	23.11	µm	23.11	µm
96	18	1067.8	µm ²	6.28		23.11	µm	0	µm	23.11	µm	46.21	µm
97	19	4805.11	µm ²	1.21		98.03	µm	32.68	µm	92.43	µm	92.43	µm

Figure 6.5 Example Screen Shot of Measurement Information.

As seen in Figure 6.4 and 6.5, the display window shows a lot of information regarding each measured object within the analysis area. The first column shows the individual number of each object, which was assigned by the software beginning in the upper left-hand corner of the counted area. The second column shows the measured area of each individual object. The third column is the measured circularity, as previously discussed. The fourth and fifth columns show the maximum and minimum diameter respectively. The next two columns refer to the horizontal and vertical Feret diameter. A Feret diameter is defined as the maximum horizontal or vertical measurement. Therefore, each measurement only refers to horizontal or vertical distance. This is particularly helpful when the object does not have perfect circularity. Additional information can also be displayed such as the perimeter of each object and the area ratio with reference to the specific area measured (not shown in Figure 6.5). Lastly, the display window shows the total object count, the total area of the objects counted and measured, total area assessed, and the ratio (in percent) between the objects counted and measured and the area assessed. The units can be changed to whatever the operator desires and defaults to the micron scale, which is observed in Figure 6.4. Once the operator inputs their desired parameter constraints, and reviews the assessment, the final area ratio value can be used as the hardened air void value.

The image shown in Figure 6.4, is an analysis of a small area of a 2% air sample, and not a complete analysis, however it is indicative of a full analysis and shows an area ratio value of 1.25% which is near the ASTM C231 measured air value of 2%. The counting and measuring software can display other information about each measured object, such as first and second moment of inertia, but the ones listed are the only ones relevant to a hardened air void analysis. Beyond specific data, the software can also present a histogram of the measured objects, which could be useful in a hardened air void analysis to assess the size variance of the air voids. Additionally, the operator can do a split screen with up to four images, that

can show the original image, the counted and measured objects, the individual object window, and the histogram plot. An example of this can be seen in Figure 6.6.

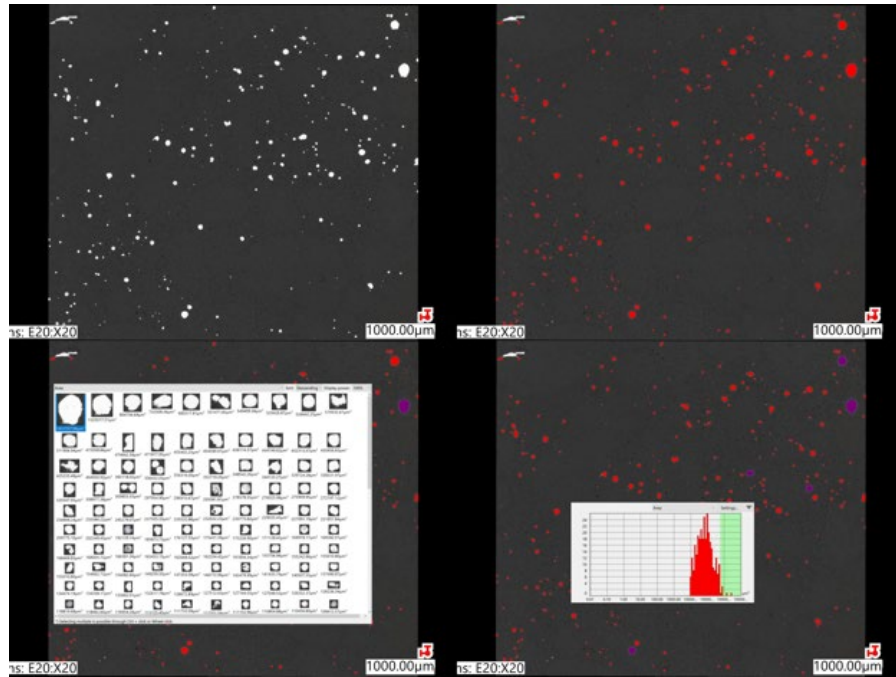


Figure 6.6 Split Window View on Keyence Microscope.

The split window view shown in Figure 6.6 can be a very useful tool when assessing the air voids in a concrete sample. Additionally, the user can highlight a specific region within the histogram plot, and those specific objects will be highlighted on the sample image. An example of this can be seen in the bottom right-hand image within Figure 6.6. The green bar on the histogram indicates the area of interest highlighted on the histogram, and behind the histogram, one can see the objects/air voids that have been highlighted in purple. Following a complete assessment, the operator can capture images at varying magnification, and in any split window configuration, as well as download all of the data into a .csv file, which can be opened and manipulated in an electronic spreadsheet.

One last feature of the Keyence – VHX 7000 microscope system is that it records and remembers all operator input settings. Therefore, upon initial use of the microscope, the operator can configure the ideal lighting, ideal magnification, and all of the counting and measuring constraints, such as minimum and maximum size, circularity, etc. Once all of this information is input, the template can be saved and anytime a new analysis is required, the original image can be opened and all of the settings can be set, based off of that image, automatically. The user does not need to individually look up each setting and manually set those values, the microscope will do all of it automatically. This feature means that any operator at any time can complete a consistent analysis at any time. This feature also extends to any other laboratory who has a Keyence VHX 7000 microscope system, as that original file can be emailed to that laboratory, and opened on that system (this feature is only compatible with the same series (i.e., 7000 series microscope). At that point, the settings can be extracted in the same manner. This feature can be used to establish interlaboratory consistency amongst all members of the NRRRA. Opening and accessing the emailed file is

also simple as the Keyence – VHX 7000 microscope system has Windows 10 installed, Wi-Fi, Bluetooth, and many other abilities like any other computer.

6.3 BRIEF SUMMARY OF ALTERNATIVE ANALYSIS PROCEDURES

The full alternative hardened air void analysis procedures can be found in Appendix A.2. However, for added clarity for the following sections a brief summary of the alternative hardened air void analysis procedures are described below:

- Place a contrast enhanced sample on the microscope system’s stage.
- Complete an “initial analysis” with only circularity constraints to obtain air void percentage value.
 - The initial analysis is completed with no size constraints (only circularity constraints) to count and measure all air voids found in the sample that are relatively circular. All non-circular items are excluded as they are not deemed an air void.
- Complete a “secondary analysis” with size and circularity constraint to obtain key calculation parameters (discussed further in Section 6.4.1).
 - Thoroughly discussed in Section 6.4.2, the hardened air void parameter, such as spacing factor and specific surface specifically depend upon the entrained air voids, not the entrapped air voids. Therefore, the secondary analysis only counts air voids within a specific size range in order to eliminate the entrapped air voids from the analysis.

6.4 CALCULATIONS AND RESULTS

6.4.1 Calculations

As discussed in Section 6.2, the standard counting and measuring assessment is able to produce the hardened air void percentage via the area ratio value. In addition to this value, the results from the assessment can be used to calculate the spacing factor and the specific surface values. This was accomplished by utilizing Equations 9, 11, 12, and 13 from ASTM C457-16 [11]. For consistency, this report will refer to these equations by their ASTM C457-16 equation number as opposed to assigning them new numbers. The first of the equations, Equation 9, can be seen below

$$\alpha = \frac{4N}{T_a} \quad \text{Eq. 9}$$

where α is the specific surface, N is the total number of air voids intersected, and T_a is the traverse length through air. In this instance, the value of N can be the total object count and T_a can be the total horizontal Feret diameter from the Keyence counting and measuring assessment. As opposed to both ASTM C457 Procedure A and B, where air voids can be missed simply due to the inherent nature of the procedure, or they can also be excluded from analysis by the operator’s opinion, this analysis would include all air voids that are within the established constraints. Additionally, using the Feret diameter would be as though a

Procedure A traverse line is passing directly through the middle of all air voids, as opposed to an area above or below the exact center of an air void, which would only partially include the air void in the analysis. As seen in Equation 9, these values can be used to calculate the specific surface of the concrete sample. This value is calculated first, as it may be required in the spacing factor calculation. The next value that is required in the calculation is the Paste-Air Ratio (p/A), which can be calculated from Equation 11

$$\frac{p}{A} = \frac{T_p}{T_a} \quad \text{Eq. 11}$$

where p is the paste content in %, A is the Air Content in %, and T_p is the traverse length through the paste. As seen in Equation 11, either side of the equation can be used to determine the Paste-Air Ratio. From the Keyence counting and measuring assessment, the air content can be extracted as the area ratio value (as previously discussed) and the paste content can be extracted from the mixture design. With these two values the Paste-Air Ratio can be determined. Once this is determined, Equation 11 can also be used to back calculate T_p by multiplying the Paste-Air Ratio by T_a , which was previously obtained to calculate the specific surface. This step is necessary for future calculations. The next step in the procedure is to compare the Paste-Air Ratio value to that of 4.342. If the Paste-Air Ratio value is less than or equal to 4.342, Equation 12 can be used to determine the Spacing Factor, if the Paste-Air Ratio is greater than 4.342 then Equation 13 should be used to calculate the Spacing Factor. Equation 12 and 13 can be seen below

$$\bar{L} = \frac{T_p}{4N} \quad \text{Eq. 12}$$

$$\bar{L} = \frac{3}{\alpha} \left[1.4 \left(1 + \frac{p}{A} \right)^{1/3} - 1 \right] \quad \text{Eq. 13}$$

where \bar{L} is the Spacing Factor (all other variables have been previously defined above). To assist with this analysis an electronic spreadsheet (Microsoft Excel™ in this study) file calculator has been developed and is provided with this document. A screencap of the excel calculator can be seen in Figure 6.7.

Total Air Void (N) [Count from Keyence Analysis]	304
Traverse Length Through Air Void [Total Feret Diameter Horizontal from Keyence Analysis]	4.44 in
Specific Surface (α)	273.9 in²/in³
Paste Percent by Volume (from mix design)	27.4 %
Air Content [Area Ratio from Keyence Analysis]	1.25 %
Paste-Air Ratio (p/A)	21.92
Spacing Factor (L bar)	0.033 in

Figure 6.7 Screencap of Excel™ Specific Surface and Spacing Factor Calculator.

As seen in Figure 6.7, the calculator requires the following inputs to complete the calculations: Count value, the Total Feret Diameter (Horizontal), and the Area ratio, from the Keyence counting and measuring analysis, as well as the paste percent, by volume, from the mixture design. The function located in the Spacing Factor solution cell contains an IF/THEN statement that compares the Paste-Air Ratio to 4.342 and then uses the appropriate equation, therefore the user does not have to worry about which equation to use.

6.4.2 Results

Following the aforementioned analysis and calculation procedure, the same samples prepared in Chapter 4 and analyzed in Chapter 5 were also analyzed via a Keyence – VHX 7000 microscope. Recall that these six samples were cut from the same cylinder for sufficient surface area and consistent representation of the entire sample and sample bias. For this initial analysis, no minimum or maximum object size constraints were used, however a circularity constraint of 0.5 – 1.5 was used to remove objects that were not relatively circular. Based off of the initial trials with the microscope, objects outside of this range generally appear to be defects, cracks, or an irregularity that is not an air void or possibly an entrapped air void, which can be irregular in shape (i.e., not circular). A range is ideal over a specific value of 1.00, as the resolution of the measurement and minor imperfections in the sample preparation can affect the absolute perfectness (a value of 1.00) of the circular air void. An initial analysis was completed with no minimum or maximum diameter, to ascertain the range of visible air voids that the microscope can see (and count and measure). Due to the high quality of the Keyence microscope, the resolution, and general state-of-the art nature, it is possible that this piece of equipment could observe more air voids than a traditional microscope. The results from this initial analysis can be seen in Table 6.1.

Table 6.1 Initial Hardened Air Void Analysis Results Completed with the Keyence – VHX 7000 Microscope.

Control - ASTM C231 Measured Air Content = 1.8%, SAM No. = 0.65							
Keyence Microscope							
Polish Pad Grit Size	260µm	125µm	70µm	30µm	15µm	6µm	AVG
Air Void Content, %	1.9	2.5	2.0	2.4	2.5	2.3	2.3
Spacing Factor, in	0.0122	0.0093	0.0189	0.0110	0.0089	0.0082	0.0114
Specific Surface, in ² /in ³	642	734	582	715	749	753	696
Low Air - ASTM C231 Measured Air Content = 3.5%, SAM No. = 0.59							
Keyence Microscope							
Polish Pad Grit Size	260µm	125µm	70µm	30µm	15µm	6µm	AVG
Air Void Content, %	4.1	3.7	3.9	3.8	4.3	3.7	3.9
Spacing Factor, in	0.0066	0.0073	0.0069	0.0077	0.0061	0.0082	0.0071
Specific Surface, in ² /in ³	831	791	812	799	849	814	816
Medium Air - ASTM C231 Measured Air Content = 4.8%, SAM No. = 0.39							
Keyence Microscope							
Polish Pad Grit Size	260µm	125µm	70µm	30µm	15µm	6µm	AVG
Air Void Content, %	5.5	5.9	5.7	5.9	5.6	5.8	5.7
Spacing Factor, in	0.0050	0.0043	0.0044	0.0042	0.0052	0.0055	0.0048
Specific Surface, in ² /in ³	807	815	827	854	812	810	821
High Air - ASTM C231 Measured Air Content = 8.7%, SAM No. = 0.12							
Keyence Microscope							
Polish Pad Grit Size	260µm	125µm	70µm	30µm	15µm	6µm	AVG
Air Void Content, %	8.9	9.1	9.3	8.9	8.8	9.2	9.0
Spacing Factor, in	0.0041	0.0049	0.0038	0.0032	0.0044	0.49	0.0041
Specific Surface, in ² /in ³	1665	1612	1691	1711	1698	1672	1675

As seen in Table 6.1, the system is able to produce hardened air void results. The hardened air void percentage determined from the system was very similar to that of the fresh air void percentage determined from ASTM C231, as well as both ASTM C457 procedures. Similar to the ASTM C457 results, it can also be observed that the air void percentage did not significantly change across the different polish pad grit sizes. One thing to note, however, is that the spacing factor values are lower than expected for the respective hardened air void values [11,13,27,33,34]. Similarly, the specific surface values are higher than expected. It is important to note, that the hardened air void values determined from those references were produced with ASTM C457 procedures, and the values shown in Table 6.1 are the first measurements produced from the Keyence microscope with no minimum or maximum object size constraints used. Therefore, the inherent issues with the ASTM C457 procedures exist with hardened air void values presented from the literature.

As previously discussed, the primary issue with ASTM C457 Procedure A and B is that both procedures can completely ignore air voids if the linear traverse line does not pass over them, or if the pre-determined stop does not stop in an air void. Additionally, the human error is still present, such that the operator has to make critical judgement calls as to when and where an air void starts or begins, or whether the pre-determined stop lands in an air void or the paste. In contrast to that, the Keyence analysis counts all objects in the pre-established counting and measuring area within the constraints established by the

operator. This results in a high object count that appears in ASTM C457-16 Equation 9 and 12. In Equation 9, N (number of air voids or measured objects) is in the numerator and in Equation 12, N is in the denominator, therefore as this number gets larger, the values from Equation 9 (Specific Surface) will get larger and the values from Equation 12 (Spacing Factor) will get smaller. This is the case as the value of N can increase at a much faster rate than the other parameters in the equation, as N will increase incrementally irrespective of the size of the object, and T_p increases proportionally to T_a , and T_a increases proportionally to the size of the object.

Therefore, with a very small air void, N will increase by a value of 1, and T_a and T_p would only increase by the measured length of that air void, which would likely not be a significant increase to the total T_a and T_p values. These results are likely due to the fact that no size constraint was applied to the initial analysis in order to allow the microscope to observe all possible objects/air voids it can. Recall that only a circularity constraint of 0.5 – 1.50 was applied with no size (diameter) constraint. Based off of the results of the initial analysis, and the manner to which the spacing factor and specific surface are calculated, a secondary analysis was completed with size constraints. Both Hover [1] and Taylor *et al.* [13] state that the size of entrained air voids is in the range of 10 – 1000 μ m (0.0004 – 0.039 in.) in diameter. Objects smaller than this range are typically capillary voids, and objects above this size range are typically entrapped air voids [13]. The size and function of pore types in concrete can be seen in Table 6.2.

Table 6.2 Pore Type and Function Related to Freeze-Thaw Durability [35].

Pore Type	Diameter	Location	Effects on Freeze Thaw
Gel Pore	Intra-gel: <0.6nm	Inside C-S-H	Water in gel pores may travel into capillary pores to reduce solution concentration due to osmotic pressure
	Inter-hydrate: 0.1 - 100 nm	Space between C-S-H and CH	
Capillary Pore	Small: 2-50 nm	Between cement grains and products of hydration	Ice crystals form in capillary pores (> 50 nm) and may generate stresses that damage the paste
	Large: 1-10 μ m		
Air Voids	Entrained: 10-1,000 μ m	Between cement grains and products of hydration	Provide boundaries for water to be forced out in capillary pores due to ice formation; limit hydraulic pressure
	Entrapped: 1 mm		No effect

Based on the information from the literature, the initial analysis using the alternative digital optical microscope method was possibly counting and measuring both capillary pores and entrapped air voids, which as previously discussed will increase N in Equations 9 and 12, and produce higher than expected values for each. According to Hover [1] and Taylor *et al.* [13] the capillary pores are typically irregular in shape (i.e., not spherical), however if they are within a 0.5 – 1.5 circularity range, they are still being counted by the initial analysis. It is more likely that the entrapped air voids are being counted and measured as they tend to be more spherical in shape than the capillary pores.

Therefore, a secondary analysis using the alternative digital optical microscope method was completed in which a size (maximum diameter) constraint was applied to only count and measure objects with a diameter within a 10 – 1000 μ m (0.0004 – 0.039 in.) range. The same circularity constraint of 0.5 – 1.50

was applied in the secondary analysis as well. It should be noted that the Keyence software does not require the operator to start this analysis over from the beginning. All the operator needs to do is to open the original assessment of the desired sample and change the desired constraints to run the analysis again. There is no need to re-stitch the image or complete any other set-up. The re-analysis takes less than five minutes per sample to complete, which includes re-opening the file and setting the new maximum diameter constraints. Therefore, the analysis was completed a second time with the mentioned constrained for all samples and the obtained data was input into the Specific Surface and Spacing Factor calculator shown in Figure 6.7.

However, for this secondary assessment, the total measured Area Ratio from the initial analysis was used. Recall that this value from the analysis is equivalent to the Air Void Percentage as the analysis is done on the entire surface and the assessment is only counting and measuring the white objects, which are air voids filled with Barium Sulfate powder from section 4.1.3.4. The rationale for keeping the same Air Void Percentage from the initial analysis is that the initial analysis is likely measuring an accurate total air void percentage (which includes capillary voids, entrained air voids, and entrapped air voids), based off the comparison between both ASTM C231 and both ASTM C457 procedures and to that of the literature [11,13,27,33,34]. Also, both ASTM C231, ASMT C457, and the SAM do not distinguish between entrained and entrapped air voids, and only report total air void percentage. However, since the Keyence characterization method is counting and measuring all of the air voids in a sample and not a portion intersecting traverse lines or stops, as with procedures A and B of ASTM C457, the analysis is more realistic. Also, the Specific Surface and Spacing Factor calculator, which uses Equation 11, requires the total measured air content (A). Therefore, the Specific Surface and Spacing Factor analysis used the measured total Air Void Percentage from the initial analysis, which did not have a size constraint, but only a circularity constraint. Proceeding in this manner also yielded more realistic and comparable results to ASTM C457. By incorporating a size constraint of 10 – 1000 μ m (0.0004 – 0.039 in.) in diameter, the analysis is removing capillary voids and entrapped air voids, and only measuring the entrained air voids in this secondary analysis.

Therefore, the secondary analysis also provided a more realistic sense of the spacing factor and specific surface as they pertain to just the entrained air voids, as these air voids are the voids primarily responsible for alleviating hydraulic and/or osmotic pressure during Freeze - Thaw cycles [1-3,5-6,11,13,27,33,34]. Lastly, proceeding in this manner also better aligned with the Specific Surface and Spacing Factor calculator developed using the ASTM C457 equations, as the N value will not be very large and distort the results, as with the initial analysis. The results of the secondary analysis (which include the previously measured air void values from the initial analysis) can be seen in Table 6.3.

Table 6.3 Secondary Hardened Air Void Analysis Results Completed with the Keyence – VHX 7000 Microscope.

Control - ASTM C231 Measured Air Content = 1.8%, SAM No. = 0.65							
Keyence Microscope							
Polish Pad Grit Size	260µm	125µm	70µm	30µm	15µm	6µm	AVG
Air Void Content, %	1.9	2.5	2.0	2.4	2.5	2.3	2.3
Spacing Factor, in	0.0237	0.0189	0.0215	0.0194	0.0180	0.0209	0.0204
Specific Surface, in ² /in ³	350	329	344	392	315	371	350
Low Air - ASTM C231 Measured Air Content = 3.5%, SAM No. = 0.59							
Keyence Microscope							
Polish Pad Grit Size	260µm	125µm	70µm	30µm	15µm	6µm	AVG
Air Void Content, %	4.1	3.7	3.9	3.8	4.3	3.7	3.9
Spacing Factor, in	0.0172	0.0194	0.0199	0.0184	0.0169	0.0189	0.0185
Specific Surface, in ² /in ³	540	504	515	534	532	494	520
Medium Air - ASTM C231 Measured Air Content = 4.8%, SAM No. = 0.39							
Keyence Microscope							
Polish Pad Grit Size	260µm	125µm	70µm	30µm	15µm	6µm	AVG
Air Void Content, %	5.5	5.9	5.7	5.9	5.6	5.8	5.7
Spacing Factor, in	0.0154	0.0119	0.0142	0.0123	0.0153	0.0127	0.0136
Specific Surface, in ² /in ³	584	612	550	601	590	621	593
High Air - ASTM C231 Measured Air Content = 8.7%, SAM No. = 0.12							
Keyence Microscope							
Polish Pad Grit Size	260µm	125µm	70µm	30µm	15µm	6µm	AVG
Air Void Content, %	8.9	9.1	9.3	8.9	8.8	9.2	9.0
Spacing Factor, in	0.0089	0.0071	0.0079	0.0084	0.0074	0.0071	0.0078
Specific Surface, in ² /in ³	701	731	715	684	672	709	702

As seen in Table 6.3 the results from the secondary analysis produced results that are more in line with expected values of similar concretes analyzed and reported in the literature [27,33,34]. This result is positive and demonstrates that the Keyence VHX – 7000 series microscope system is capable of producing a hardened air void analysis on polished concrete samples. A full in-depth comparison of these results with that of the ASTM C457 results obtained in Chapter 5 will be discussed and presented in the forthcoming Chapter 7.

CHAPTER 7: RESULTS ANALYSIS AND COMPARISON

7.1 METHODOLOGY

In this study, the results of the alternative hardened air void analysis were compared to that of ASTM C457 Procedure A and Procedure B. In Chapter 5 the quality of the ASTM C457 Procedure A and Procedure B results were compared and discussed in relation to each other as well as the fresh air results from ASTM C231 and the SAM. Additional comparisons were completed and discussed regarding the polishing steps in the preparation of the hardened samples. Chapter 6 presented the results obtained from the alternative hardened air void analysis, which was obtained via a Keyence – VHX 7000 Series Digital Optical Microscope. That chapter also included the equipment and consumables required to produce an alternative hardened air void analysis, a list of the equipment and materials, procedures, calculations, and an estimate of the time to complete the alternative analysis. This chapter provides additional result analysis, comparison, and discussion.

7.2 FINAL RESULTS ANALYSIS AND COMPARISONS

As with the ASTM C457 results, the results of the alternative hardened air void analysis were compared to ASTM C231 with respect to the polish pad grit size. For reference, both ASTM C457 procedure A and B were included. The results can be seen in Figures 7.1 – 7.4.

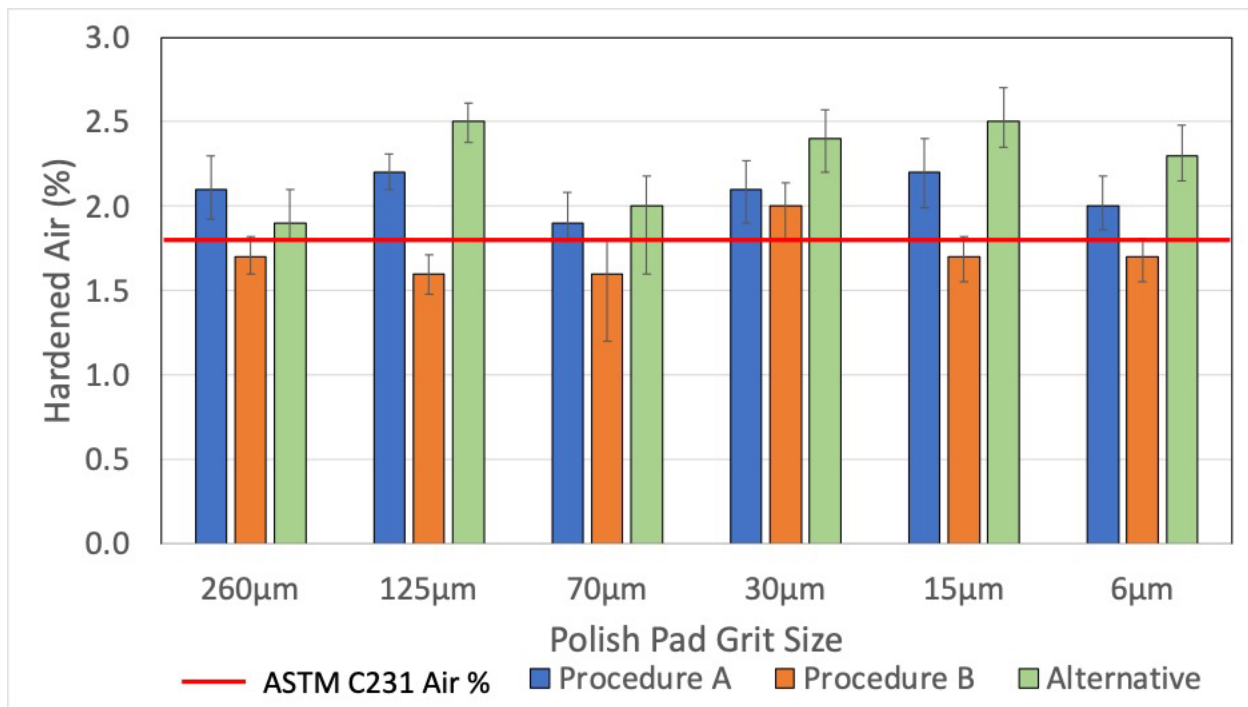


Figure 7.1 Control (2% Target) Hardened Air Void Comparison.

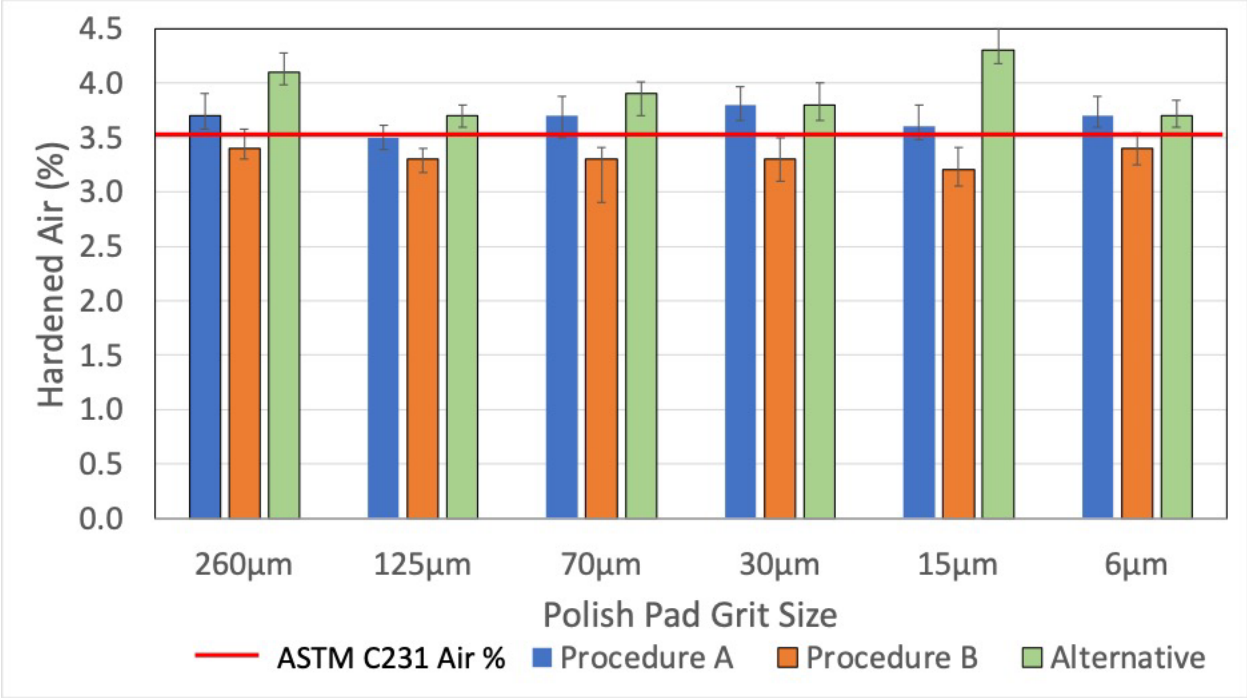


Figure 7.2: Low Air (3-5% Target) Hardened Air Void Comparison.

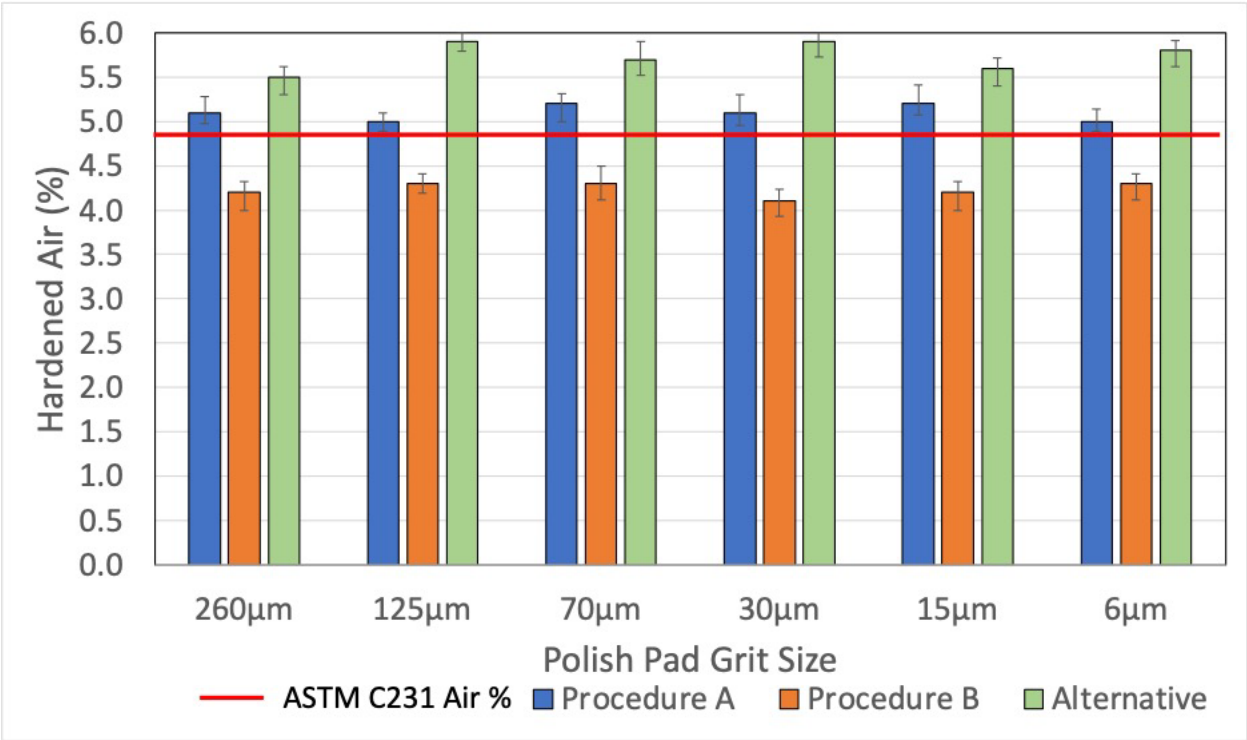


Figure 7.3: Medium Air (5-7% Target) Hardened Air Void Comparison.

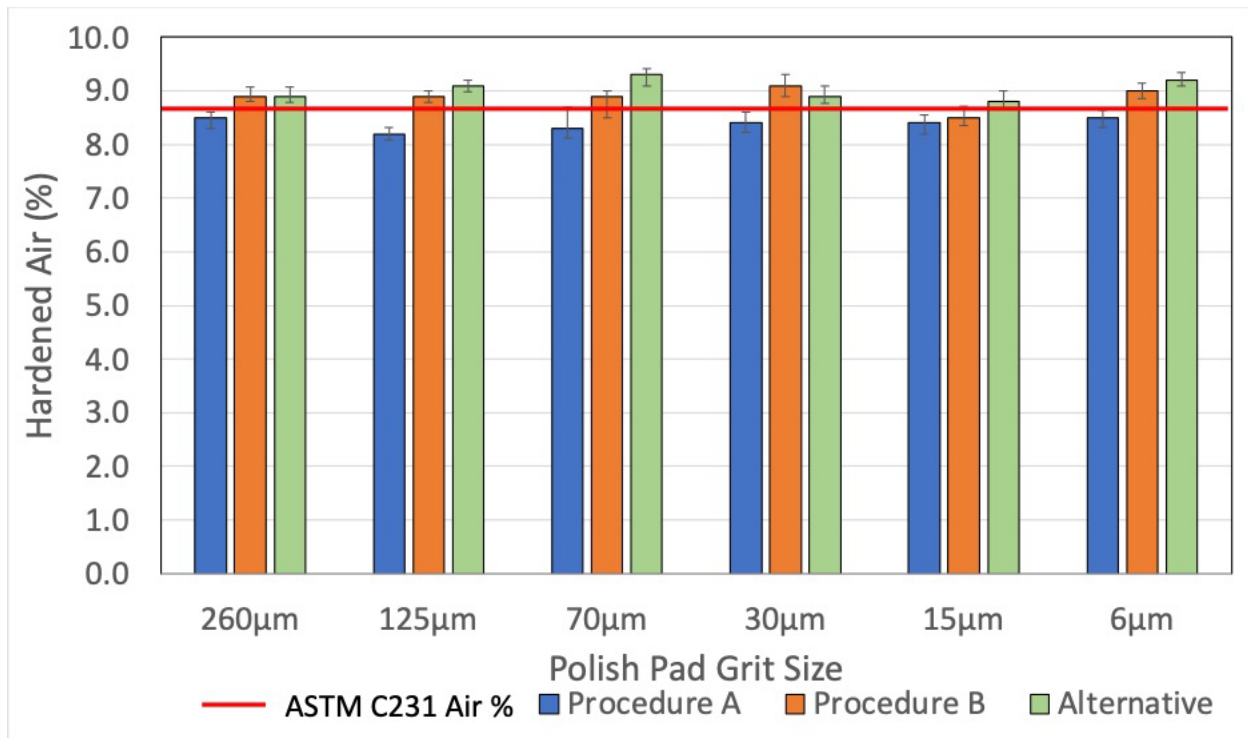


Figure 7.4: High Air (>8% Target) Hardened Air Void Comparison.

As seen in Figures 7.1 – 7.4, the alternative hardened air void analysis produces results that are similar to that of both ASTM C457 and ASTM C231, and are within expected hardened air void values based on the concrete mixture design. Within the alternative analysis results, a trend is observed. In general, the alternative analysis produces slightly higher hardened air void results than the traditional methods, especially when the air void percentage is low. This observation makes sense as one of the major issues with both ASTM C457 procedures is that both can completely skip over air voids within the analysis area, in that they are not counting all of the air voids in the specimen. Additionally, ASTM C457 states that the analysis should be distributed evenly over the sample area [11].

Therefore, with a circular cross section (like the ones used in this study), an evenly distributed analysis is not doable as the traverse lines would have uneven lengths across the sample (Procedure A) or there will be more or less pre-determined stops (Procedure B). Therefore, with a circular cross section a perfectly square area is assessed to allow for an evenly distributed analysis – i.e., the traverse lines will all be the same length or there will be an even distribution of pre-determined stops. With a 4 in. (101.6 mm) diameter concrete sample, this typically correlates to approximately 2.75 in. x 2.75 in. (70mm x 70mm) square area. This is determined geometrically, as a 2.75 in. x 2.75 in. (70mm x 70mm) is approximately the largest square that can fit in a 4 in. (101.6 mm) diameter concrete sample. These dimensions are approximate as the concrete sample itself is not perfectly 4" in. (101.6 mm) in diameter. Therefore, beyond the inherent issues with missing air voids or the possibility of user error, entire portions of the specimen are left out of the analysis. The 2.75 in. x 2.75 in. (70mm x 70mm) only represents approximately 50% of the entire sample surface, therefore approximately half of the specimen is not being analyzed. These issues are enhanced when the air percentage is lower, as the air voids are statistically unlikely to

be within a confined area, which is one of the reasons for the minimum area assessment requirement in ASTM C457 [11].

With the new alternative analysis, not only is the microscope counting and measuring all of the air voids in the sample (i.e., not skipping over any), approximately 98% of the sample surface is being assessed. Recall that portions of the sample edges are typically removed from the analysis due to imperfection from the sample cutting and polishing procedures, discussed in Appendices A.1. Therefore, with the alternative analysis over 12 in² (77.4 cm²) is assessed per sample, which is higher than the minimum assessment area required by ASTM C457 for 0.75 in. (19mm) nominal maximum sized aggregate mixtures [11]. With the traditional procedures, typically two 4 in. (101.6 mm) diameter concrete samples are required, to meet the minimum traverse area, which, at minimum, doubles the processing time. Alternatively, a larger sample could be created by cutting a 4" (dia.) x 8" (length) concrete cylinder in half lengthwise and using the approximate 4" (wide) x 8" (length) surface area. However, this sample configuration may not fit most auto-polishers and the corresponding sample holder.

Additional comparison between the alternative analysis and each ASTM C457 procedure can be seen in Figures 7.5 – 7.6.

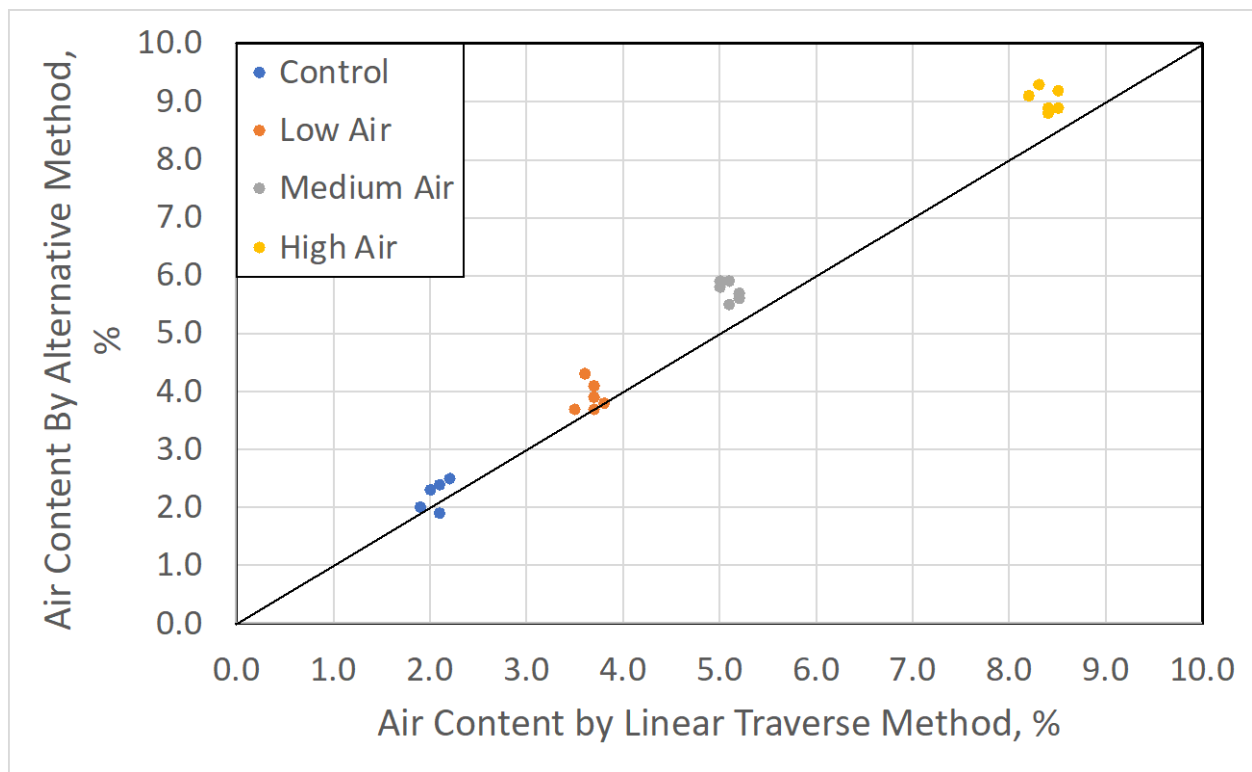


Figure 7.5: Comparison Between Alternative Method vs. Linear Traverse Method (ASTM C457 Procedure A).

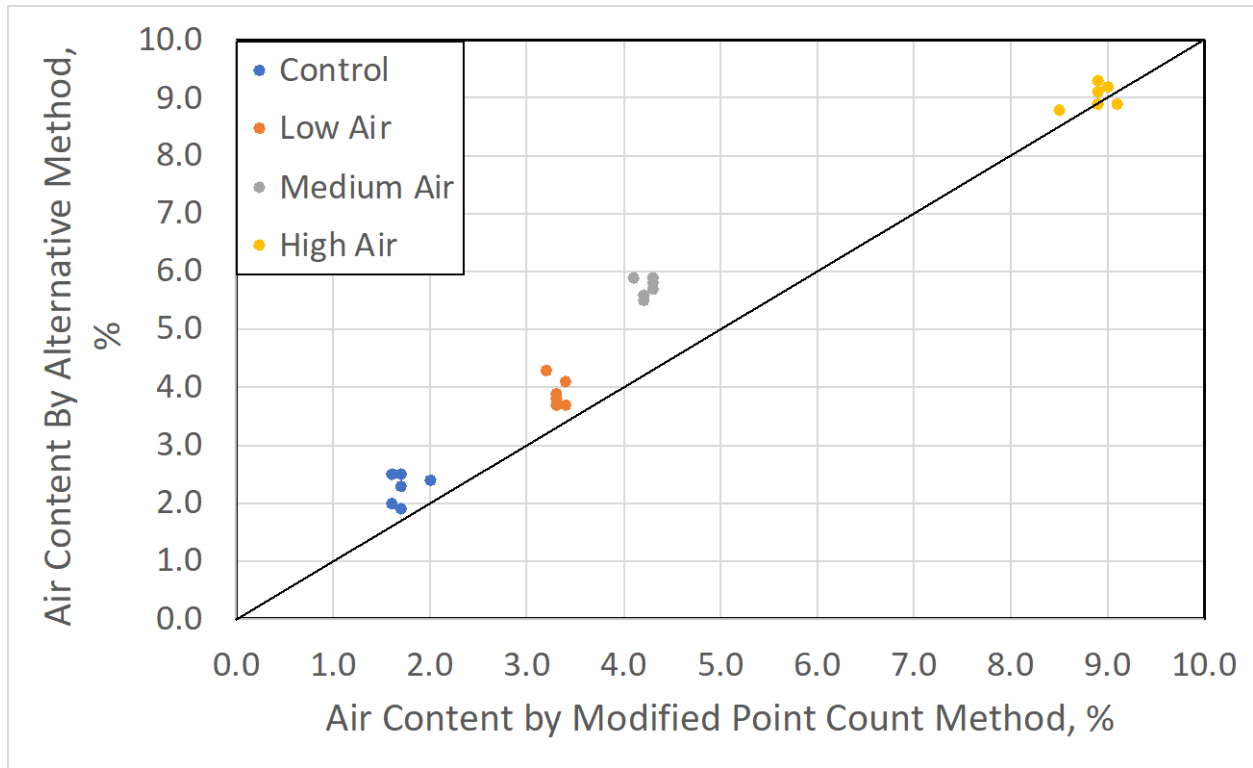


Figure 7.6: Comparison Between Alternative Method vs. Modified Point Count Method (ASTM C457 Procedure B)

As seen in both figures, the 45° line represents a “line of equality” which corresponds to a perfect agreement between the two procedures. It is observed that there is a relatively close agreement between the alternative method and the two ASTM C457 procedures. In general, the hardened air content results favor the alternative method, in that the values are slightly higher than the ASTM C457 procedures. As previously discussed, the slightly higher results from the alternative method are due to the alternative method likely counting and measuring every possible air void in the sample, and not skipping over any air voids that is very likely in the two ASTM C547 procedures.

Additionally, the alternative method has no user-bias or user-error, which produce a more realistic assessment of the hardened air voids in each sample. These slight differences also only correspond to an overall average of a 0.6 difference between the hardened air void results, with an average specific difference of 0.5 and 0.7 between the alternative method and Procedure A and Procedure B, respectively. These averages are all less than the average precision data reported in Table 4 of ASTM C457-16 [11], where the standard reports a range of air content percent of 0.82 for within lab precision and 1.16 for between lab precision. Therefore, the differences between the results are likely negligible. In order to confirm that these values are in fact negligible, a student t-test was performed on the hardened air void data with a confidence level of 0.05 (p-value). The t-test confirms that the values are not statistically significant between each other, which confirms that the differences are negligible. This demonstrates that the alternative method produces comparable results to ASTM C457, but is quicker and less reliant on human error, which leads to more reliable results.

When comparing the spacing factor and the specific surface results between the alternative method and the two ASTM C457 procedures, the outcome is similar. A comparison of the spacing factor and the specific surface results can be seen in Figures 7.7 and 7.8. The values in these figures represent the average across all of the polishing pad sizes discussed used in Chapter 4. As discussed in chapter 5 and 6, these results were statistically similar, thus representing their average for comparison is acceptable.

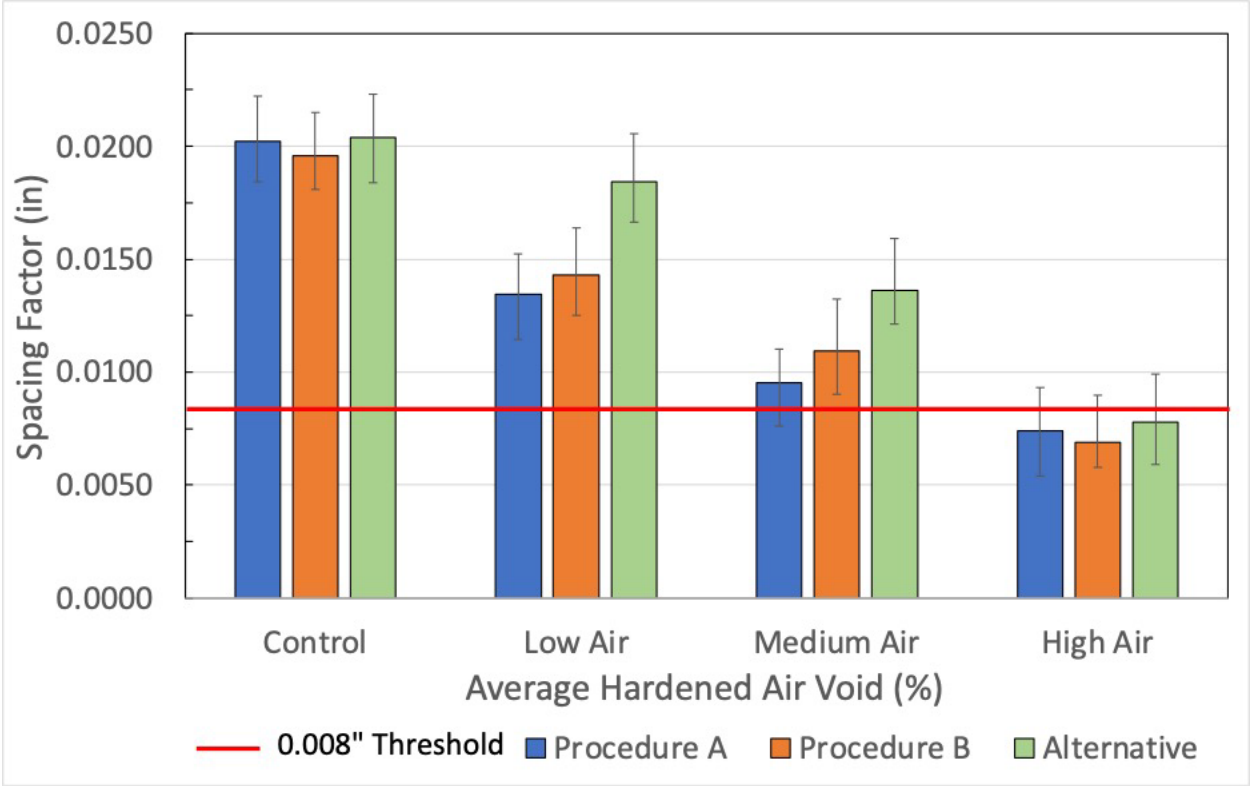


Figure 7.7: Average Spacing Factor Results for the Alternative Method and ASTM C457.

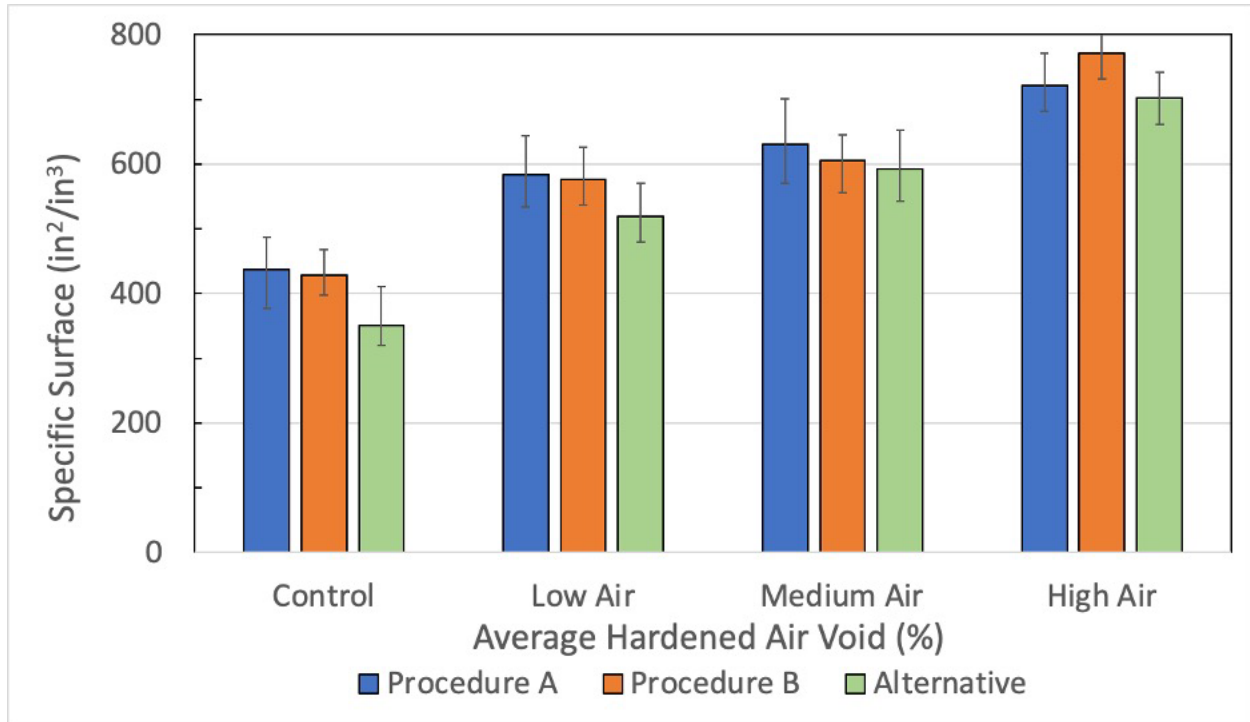


Figure 7.8: Average Specific Surface Results for the Alternative Method and ASTM C457.

As seen in Figures 7.7 and 7.8, the respective results are very comparable. Looking at the average spacing factor results, the results for each percent air are not only similar but they are as expected with reference to the literature [33-35]. It can also be observed that the high air samples were the only ones in this study to be below the 0.008 in. (200 μ m) threshold, which typically corresponds to good Freeze-Thaw durability performance. The average difference between the alternative method and ASTM C457 Procedure A and Procedure B is only 0.001 and 0.002, respectively, which is negligible. Comparing the results of the specific surface analysis also shows a similar outcome. The results are not only similar but they are also as expected with reference to similar samples assessed via ASTM C457 from the literature [33-35]. The average difference between the alternative method and ASTM C457 Procedure A and Procedure B is only 23 and 52, respectively, which is also negligible for these values. As was done with the hardened air void data, a statistical analysis was completed on both the spacing factor and the specific surface data to confirm that the differences between the results is in fact negligible. Using the same p-value, the statistical analysis revealed that the difference between each method is negligible.

Based off the results presented and discussed in chapters 5 - 6, it can be concluded that the alternative hardened air void method using a Keyence VHX – 7000 series microscope is capable of producing quality hardened air void data that is easier, quicker, more reliable, and less reliant on human decision making. Not investigated in this study, but is likely is that the analysis is repeatable and comparable between users and laboratories. To provide further context regarding the reliance to human decision making, both the alternative procedure using the Keyence digital optical microscope and Procedures A and B from ASTM C457 require the same level of human decision making when preparing the sample surfaces. If the operator chooses to contrast enhance the sample surface (which is acceptable for Procedure A and B, and

optional for the alternative method) there exist an additional level of human decision making, however, this is minimized if one follows the procedures outlined in Appendix A.2. When it comes to the actual analysis procedure itself, there is a significant degree of human decision making when performing either ASTM C457 Procedure A or B, as a decision needs to be made for every single intersection with a void (Procedure A) or every stop (Procedure B), which could be on the order of 100 to 1000s of decisions per sample. With the alternative method, the only human decision that is made (if one follows the procedures outline in Appendix A.2) is where to establish the analysis boundary, and this process could be minimized with an in-house defined procedure. After that is established in the alternative method, the entire analysis procedure is fully automated by the digital optical microscope system. Regarding calibration, both Procedure A and B and the alternative method require an initial calibration and set up of the equipment. With the Keyence digital optical microscope, the initial calibration is typically done during the set-up of the microscope with Keyence personnel, but if calibration is needed in the future, the Keyence microscope is self-calibrating. All a user needs to do is place the calibration slide on the microscope stage, select auto-focus, select calibrate, and the software will self-calibrate without the need for human intervention.

CHAPTER 8: CONCLUSIONS AND RECOMMENDATIONS

8.1 INTRODUCTION

In this chapter, the major conclusions and recommendations are discussed as they relate to the benefits of adapting the alternative method. Additionally, this chapter discusses the methodology for implementation, steps and approach for evaluating benefits (both quantitative and qualitative), and a discussion of next steps for implementation are prepared and discussed.

8.2 MAJOR CONCLUSIONS AND RECOMMENDATIONS

The major conclusions from the study are as follows.

1. All concrete mixtures produced in this investigation contained as expected fresh and compressive strength data, relative to the four target air contents investigated.
2. Discoveries related to the preparation of the hardened concrete sample for evaluation are as follows:
 - The diamond cut off blade produced superior saw cuts on the concrete cylinders, which significantly reduced the subsequent polishing steps. This was compared to a conventional concrete laboratory saw.
 - Diamond metal backed polishing discs last longer and reduce the polishing time significantly as compared to traditional silicon carbide paper polishing discs when used to polish hardened concrete samples.
 - The first polishing step, using the coarsest polishing medium, is the most crucial step in producing a suitable surface, on hardened concrete samples for further analysis. In this first step it is critical to achieve an entirely flat polished surface.
 - The research shows that once an entirely flat surface is achieved with the 260 μ m disc, no additional polishing is necessary. The results from polishing other samples using subsequent polishing pad grit size of 125 μ m, 70 μ m, 30 μ m, 15 μ m, and 6 μ m are unnecessary for the alternative method of analysis and likely ASTM C457 as well.
 - When contrast enhancing a sample, using a water soluble black acrylic ink and a rubber roller is preferred over a black marker.
 - The preferred white powder used to fill air voids in the sample is barium sulfate.
3. The results showed an average hardened air void difference of 0.5% and 0.7% between the alternative hardened air void analysis method and ASTM C457 Procedure A and Procedure B, respectively.
4. The results shown an average air content difference of 0.5% between the alternative hardened air void analysis method and the fresh air content determined with ASTM C231.
5. The results also showed a reduction of time: From an estimated 2 - 4 hours/sample (ASTM C457) down to an estimated 15 minutes/sample (alternative method).

8.3 METHODOLOGY FOR IMPLEMENTATION

The recommended methodology for implementing the alternative hardened air void analysis procedure in ones' laboratory is as follows:

1. Review the information found in this report.
2. Purchase and acquire suitable equipment and tools as outlined in this report.
3. Utilize tutorials associated with the chosen digital optical microscope system.
4. Once the equipment and tools are acquired and set up, follow the procedures outlined in Appendix A.1 and A.2 of this report to prepare each sample, then follow the procedures outlined in chapter 6 to complete the alternative hardened air void analysis.
5. Analyze and or report hardened air void results.

8.4 STEPS AND APPROACH FOR EVALUATING BENEFITS (BOTH QUANTITATIVE AND QUALITATIVE)

8.4.1 Quantitative Result Benefits

8.4.1.1 Test Time

To evaluate the benefit from a reduced testing time, an evaluator would need to compare the time it takes to assess a prepared hardened concrete sample using ASTM C457 (Procedure A and Procedure B) to that of the alternative method. Preparation of the sample is the same process for both methods, when completing a time comparison analysis. It should be mentioned that the contrast enhanced procedure is not necessarily required for ASTM C457 Procedure A and B, but is required for the alternative method. Therefore, it may also be necessary to evaluate the time it takes the same or multiple operators to complete the contrast enhanced procedure.

8.4.1.2 Acceptable Results or Variation in Results

To evaluate the benefit from the alternative method producing similar results to ASTM C457 (Procedure A and Procedure B), an evaluator would compare the results obtained from both methods. This can be executed in a computer program or electronic spreadsheet in which commands such as average, percent difference, standard deviation, and other statistical analysis could be completed.

A list of quantitative results from using the alternative hardened air void analysis method are as follows:

- Sample preparation, including sawing, polishing, and contrast enhancement following the procedures outlined in Appendix A1 should take between 20 minutes and 1 hour.
- Completing an alternative hardened air void analysis using the digital optical microscope system should take between 10 and 30 minutes.
- The hardened air void percentage should be within $\pm 1\%$ of the fresh air void content as determined by ASTM C231.

- The specific surface and spacing factor should be within $\pm 8\%$ and $\pm 4\%$ respectively when compared to ASTM C457 Procedure A and B.

8.4.2 Qualitative Results Benefits

To evaluate the qualitative benefits, a user would have to complete an analysis using the alternative method using a digital optical microscope system. The user would determine the extent of the benefits from a reduction in human decision making and how intuitive the microscope software is to operate. To fully realize the benefits, more than one analysis is recommended, as one of the qualitative benefits is that once the initial testing parameters are established, the entire process becomes even more streamlined and easy to execute. Additional benefits can be realized by other agencies completing the same procedures and parameters established from an entirely different agency, in which they would benefit from the established streamlined procedures.

A list of qualitative results to be determined include:

- Are human decision-making errors reduced?
- Are the results more reliable?
- Can the reduced testing time allow operators to execute more tests per day or to focus on other daily activities?
- Is the process less stressful for the operator?
- Can the procedure be saved on the microscope system for ease of repeatability?
- Can the saved procedure be transferred to all who own the same model of microscope?
- Can the microscope system be used for other microscope and counting/measuring analysis beyond hardened concrete air void analysis?

8.5 DISCUSSION OF NEXT STEPS FOR IMPLEMENTATION

The discussions for next steps for implementation are broken up into two sections; i) a discussion on considerations related to the alternative hardened air void method discussed in this research and ii) a discussion on considerations related to determining both fresh and hardened air void characterization in general.

8.5.1 Considerations Related to the Alternative Hardened Air Void Analysis Method

The following are a list of considerations for further validation of the alternative hardened air void analysis method using a digital optical microscope system.

- Explore various concrete mixture designs and constituents (cement type/content, water-to-cement ratio (w/c), supplementary cementitious materials (SCMs), various aggregates (including lightweight aggregate), various admixtures, etc.) including job-based mixtures during field placements.
- Perform a comparison between field fabricated samples during placement and cores taken from hardened concrete structure.

- Try larger sized hardened samples, such as cutting a 4" (dia.) x 8" (length) cylinder lengthwise to create a rectangular sample of approximate dimensions 4" (wide) x 8" (length).
- Perform comparisons to the automated RapidAir 457 device, which also requires the samples to be contrast enhanced.
- Validate and develop precision and bias data for alternative method through other operators and/or other laboratories.

8.5.2 Considerations on General Fresh and Hardened Air Void Analysis

8.5.2.1 Fresh Concrete Air Void Analysis Using Super Air Meter

During the course of this investigation, the participants discovered many issues when performing the SAM test. It was learned that if not all air was removed from the headspace between the base (unit weight bucket) of the SAM and the top, then the user would receive an error. Also, if there is air remaining, and the user does receive SAM results, those results can be skewed by the remaining air in the headspace. In its current state, it is impossible to determine when the headspace is completely empty of air. The current recommendations to minimize this issue is to either use the "shotgun funnel" and/or run multiple tests to obtain an average. Shipped along with the SAM is a black funnel colloquially known as a "shotgun funnel" or simply the "shotgun" that can be affixed to one of the petcock valves. If the operator fills this funnel with water, and tips the SAM while opening the petcock valves, the water from the funnel will rapidly fill the headspace while pushing out the air from the other petcock valve. It is also advised that the operator hit the side of the base with the mallet while performing this procedure to "knock" out any of the air bubbles. Although some users have success with this method, there is an inherent issue in the testing method when the procedure relies on human execution, especially when that execution can have a strong influence on the results.

One proposed idea to solve this issue is to develop a device that can be connected to one end of the petcock valve, when the shotgun funnel is connected to the other petcock valve. The newly developed device can contain a pressure gauge, valves, and a handled "bulb" (similar to a blood pressure cuff) that can be squeezed to completely, uniformly, and reliably remove all air from the headspace before it is filled with water. A small air pump could also be incorporated if needed. This would drastically reduce the human error variable in order to produce more reliable SAM values. The objective of the research would be to develop and calibrate the device with a focus on minimizing cost, procedure time, and validating the data.

8.5.2.2 Hardened Air Void Analysis

It is of the authors' opinion that Artificial Intelligence (AI) and Machine Learning (ML) could be used to simply bypass any hardened air void analysis entirely. This unique and cutting-edge approach could be developed to be accurate, reliable, and significantly reduce testing time to determine all hardened air void parameters. This could be executed by first building a database of input parameters to train the AI to learn about the input parameters and desired output values. The input parameters would be mixture design

information, fresh concrete data, and hardened air void data. The training data can come from current published literature, DOT/NRRA reports, and newly obtained data (if needed).

The framework of this idea is that ML (a specifically developed computer program) uses past data to learn upon its “experience” to predict what the output would be from new information. ML works by exploring data, correlation, and identifying patterns to reduce human intervention and accurately predict what the results would be of a similar scenario. This process can be seen in Figure 8.1.

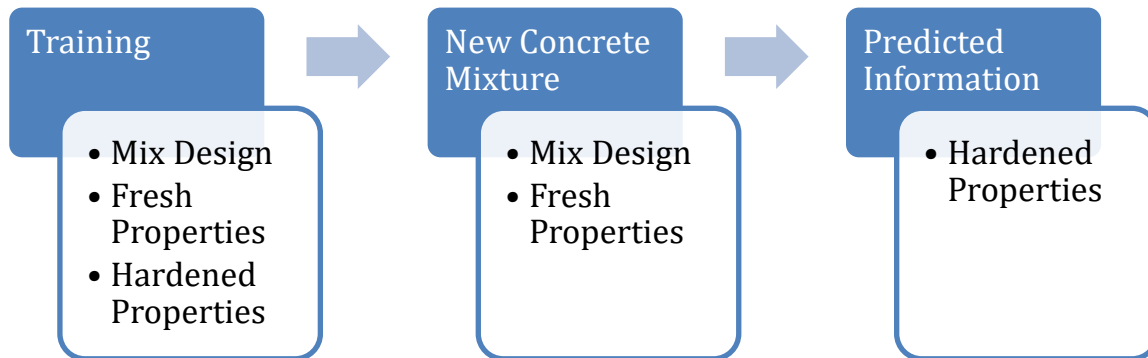


Figure 8.1 Machine Learning Process for Hardened Air Void Analysis.

As seen in Figure 8.1, the process would involve first training the AI program to learn about the input values. The more information put into the training data phase will result in more accurate predicted data. Once the AI is trained, information from any new concrete mixture can be put into the program, and without actually performing any hardened air void testing, the AI will predict what the hardened air void parameters will be. Therefore, if NRRA members have a site pour scheduled, all they would need to do is to input mixture design variables, slump, unit weight, and air content, which are already typical on-site testing procedures. Then the AI will accurately determine the hardened air void parameters, which would completely eliminate the need to perform these tests. The objective of this research would be to develop the AI, train the AI, and iteratively validate and adjust the AI for accuracy. The end result of the AI can then be packaged into a simple to use phone application or website with easy-to-use input windows.

This type of research has already shown success in the cement and concrete research arena by drastically reducing large testing matrices. Moro *et al.* (2021) [36] used an AI, written in MATLAB, to predict the compressive strength of mortars based on five different properties. Therefore, for each mixture (data from literature), they had five inputs: (1) % of nano- TiO₂, (2) testing age, (3) a/b ratio, (4) w/b ratio, and (5) cement content and they were able to obtain the predicted compressive strength of the mortars using those variables. Then the authors were able to manipulate the input parameters in order to artificially determine the impact of said manipulation without physically testing the thousands of possible combinations. Once a desired manipulation is determined, the authors casted and tested those mortars to confirm the data, based on empirical evidence, in which the empirical data often correlated with the AI predictions [36].

REFERENCES

- [1] Hover, K.C., "Air Content and Density of Hardened Concrete," STP169D - Significance of Tests and Properties of Concrete and Concrete-Making Materials, Eds. Lamond, JF, Pielert, JH, Chapter 26, pp. 288-309, 2006
- [2] Powers, T. C., "A Working Hypothesis for Further Studies of Frost Resistance of Concrete," Journal, American Concrete Institute, Feb. 1945; Proceedings, Vol. 41, pp. 245–272
- [3] Powers, T. C., "The Air Requirement of Frost-Resistant Concrete," Proceedings, Highway Research Board, Vol. 29, 1949, pp. 184–202.
- [4] Powers, T. C., "Void Spacing as a Basis for Producing Air Entrained Concrete," Journal, American Concrete Institute, May 1954; Proceedings, Vol. 50, pp. 741–759.
- [5] Powers, T. C. 1954. Void Spacing as a Basis for Producing Air-Entrained Concrete. Research Bulletin 49, Portland Cement Association, Journal of the American Concrete Institute, pp. 741–760.
- [6] Powers, T. C. 1955. Resistance to Weathering—Freezing and Thawing in Significance of Tests and Properties of Concrete and Concrete Aggregates. ASTM STP 169. American Society for Testing and Materials, West Conshohocken, PA.
- [7] Powers, T. C. 1958. Structure and Physical Properties of Hardened Portland Cement Paste, Journal of the American Ceramic Society, Vol. 41, No. 1.
- [8] Powers, T. C. 1960. Physical Properties of Cement Paste. Proceedings of the Fourth International Symposium on the Chemistry of Cement, pp. 577–613.
- [9] Powers, T. C. 1968. Properties of Fresh Concrete. John Wiley & Sons, Inc., New York, NY. Powers, T. C. 1975. Freezing Effects in Concrete, Durability of Concrete. SP-47, pp. 1–11. American Concrete Institute, Farmington Hills, MI.
- [10] Natesaiyer, K. C. and Hover, K. C., "The Protected Paste Volume of Air Entrained Cement Paste, Part I," Journal of Materials in Civil Engineering, Vol. 4, No. 2, May 1992, pp. 166–184.
- [11] ASTM Standard C457/C457M - 16, "Standard Test Method for Microscopical Determination of Parameters of the Air-Void System in Hardened Concrete" Annual Book of ASTM Standards, Vol. 09.49, ASTM International, West Conshohocken, PA
- [12] Brown, L. S. and Pierson, C. U., "Linear Traverse for Measurement of Air in Hardened Concrete," Proceedings, American Concrete Institute, Vol. 47, 1950, pp. 117–123.
- [13] Taylor, P., Sadati, S., Wang, K., Ling, Y., Wang, X., Sun, W., Kevern, J. T., & Ryazi, S. (2021). Entrained Air-Void Systems for Durable Highway Concrete. <https://doi.org/10.17226/26071>

- [14] Cordon, W. 1966. Freezing and Thawing of Concrete Mechanisms and Control. Monograph No. 3. American Concrete Institute, Farmington Hills, MI.
- [15] Jennings, H. M., J. W. Bullard, J. J. Thomas, and J. E. Andrade. 2008. Characterization and Modeling of Pores and Surfaces in Cement Paste: Correlations to Processing and Properties. *Journal of Advance Concrete Technology*, Vol. 6, No. 1, pp. 5–29.
- [16] Verbeck, G. and P. Klieger. 1956. Studies of “Salt” Scaling of Concrete. Bulletin No. 150. Highway Research Board, Washington, DC.
- [17] Aligizaki, K. K. 2006. Pore Structure of Cement-Based Materials: Testing, Interpretation and Requirements. Taylor & Francis, New York, NY.
- [18] Akyurt, M., G. Zaki, and B. Habeebullah. 2002. Freezing Phenomena in Ice-Water Systems. *Energy Conversion and Management*, Vol. 43, No. 14, pp. 1773–1789.
- [19] Fagerlund, G. 1993. The Long-Time Water Absorption in the Air-Pore Structure of Concrete.
- [20] Li, W., M. Pour-Ghaz, J. Castro, and J. Weiss. 2012. Water Absorption and Critical Degree of Saturation Relating to Freeze-Thaw Damage in Concrete Pavement Joints. *Journal of Materials in Civil Engineering*, Vol. 24, No. 3, pp. 299–307.
- [21] Plum, D. R. and Hammersley, G. P. 1984. Concrete Attack in an Industrial Environment. *Concrete*, Vol. 18, No. 5, pp. 8–11.
- [22] AASHTO T 152 Standard Method of Test for Air Content of Freshly Mixed Concrete by the Pressure Method. 2017. American Association of State Highway and Transportation Officials, Washington, DC.
- [23] Lamond, J. F. and J. H. Pielert, Editors. 2006. Significance of Tests and Properties of Concrete and Concrete-Making Materials. STP 169D. Issue 169, Part 4. ASTM International, West Conshohocken, PA.
- [24] Sutter L. L. 2007. Evaluation of Methods for Characterizing Air-Void Systems in Wisconsin Paving Concrete. Wisconsin Highway Research Program, Madison, WI.
- [25] Kozikowski, R. L., Jr., D. B. Vollmer, P. C. Taylor, and S. H. Gebler. 2005. Factors Affecting the Origin of Air-Void Clustering. PCA R&D Serial No. 2789. Portland Cement Association, Skokie, IL.
- [26] Riding, K. A., A. Esmaily, and J. Vosahlik. 2015. Air Void Clustering. Kansas State University Transportation Center and Kansas Department of Transportation, Manhattan and Topeka, KS.
- [27] ACI Committee. 201, 201.2R-16: Guide to Durable Concrete; American Concrete Institute: Michigan, MI, USA, 2016.
- [28] Ley, T. and Tabb, B., “Development of a Robust Field Technique to Quantify the Air-Void Distribution in Fresh Concrete,” Publication No. DTRT06-G-0016, Oklahoma Transportation Center, Stillwater, OK, 2013.

- [29] Ley, M. & Welchel, David & Peery, Jacob & LeFlore, Jake & Khatib, Morteza. (2017). Determining the air-void distribution in fresh concrete with the Sequential Air Method. *Construction and Building Materials*. 150. 723-737. 10.1016/j.conbuildmat.2017.06.037.
- [30] Fonseca, P.C., Scherer, G.W. An image analysis procedure to quantify the air void system of mortar and concrete. *Mater Struct* 48, 3087–3098 (2015). <https://doi.org/10.1617/s11527-014-0381-9>
- [31] Carlson, J. & Sutter, Lawrence & Peterson, Karl & Van Dam, Thomas. (2005). An update on application of a flat-bed scanner for performing ASTM C 457. 27th International Conference on Cement Microscopy 2005.
- [32] Chatterji S, Gudmundsson H (1977) Characterization of entrained air bubble systems in concretes by means of an image analyzing microscope. *Cem Concr Res* 7:423–428
- [33] Ley, T., Felice, R., and Freeman, J.M., “Concrete Pavement Mixture Design and Analysis (MDA): Assessment of Air Void System Requirements for Durable Concrete” A report from National Concrete Pavement Technology Center prepared for the Federal Highway Administration (FHWA), DTFH61-06-H-00011 Work Plan 25, June 2012
- [34] Pham, L. and Cramer, S., “Comparison of Fresh Concrete Air Content Test Methods & Analysis of Hardened Air Content in Wisconsin Pavements” Final Report to Wisconsin Department of Transportation Hill Farms Building, WHRP 0092-14-05, February 2019
- [35] Mehta, P. K. 1986. *Concrete: Structure, Properties, and Materials*. Prentice-Hall, Englewood Cliffs, NJ.
- [36] Moro, C. El Fil, H., Francioso, V., Velay-Lizancos, M., “Influence of water-to-binder ratio on the optimum percentage of nano-TiO₂ addition in terms of compressive strength of mortars: A laboratory and virtual experimental study based on ANN model”, *Construction and Building Materials*, Volume 267, 2021

APPENDIX A

A.1 SAW CUTTING MATERIALS, EQUIPMENT, AND PROCEDURES

Table A.1 lists the materials and equipment that are currently available and were used for the saw cutting procedure.

Table A.1 Saw Cutting Materials and Equipment

Item	Estimated Cost
Wet Saw	\$5,000
Saw Blade	\$300
C-Clamp	\$20

A.1.2 Saw Cutting Procedures

1. With a diamond cut off blade to the wet saw.
2. Place a 4" (diameter) x 8" (length) concrete cylinder on the rolling carriage tray on the wet saw.
 - a. The concrete cylinder should be up against the rear guide bar, along its long axis.
3. Measure the desired sample thickness by either marking the sample or measuring from the outer edge of the saw blade to the edge of the sample.
4. Once the concrete cylinder is in the desired location, use a c-clamp to secure the cylinder in place ensuring the clamp arm is out of the path of the blade, as seen in Figure A.1.



Figure A.1 Concrete cylinder mounted to wet saw.

5. Before cutting, ensure that the blade is approximately 1/4" below the rolling carriage tray into the cutting groove. This will ensure the blade cuts all the way through the concrete cylinder.
6. Turn the wet saw on, and slowly move the carriage tray towards the blade to begin cutting.
7. Continue pushing the carriage tray towards the saw blade at a slow pace throughout the entire cut, until the cut is complete.

8. Following cutting of the cylinder, select samples in accordance to ASTM C457 sampling section (Section 7 of ASTM C457).
 - a. For the purposes of this study, all sawn surfaces were polished for further investigation.

A.1.3 Polishing Materials and Equipment

Table A.2 lists the materials and equipment currently available and were used for polishing procedure.

Table A.2 Polishing Materials and Equipment.

Item	Estimated Cost
Auto-Polisher	\$5,000
Diamond Polishing Pad	\$600/disc
Crayons	\$5

The specific auto-polisher model used in this study is a standard auto-polisher used for these types of applications. It is important to note that an appropriate sample holder fixture is needed for this process. The one used in this study was produced in house. To the authors' knowledge, the manufacture of the polisher will work with new clients to develop an appropriate sample holder for the new user's needs. Manufacturers also may have sample holders available to purchase.

A.1.4 Polishing Procedures

1. Prior to polishing a sample surface use a crayon to draw a grid on the surface spaced approximately $\frac{1}{4}$ " x $\frac{1}{4}$ " as seen in Figure A.2. This is necessary to help determine if the specimen surface is polished completely flat.
 - a. The lines do not have to be perfectly straight or perfectly spaced, but choose a color that contrasts with all features on the sample surface.
 - b. This is best completed on a dried sample surface.

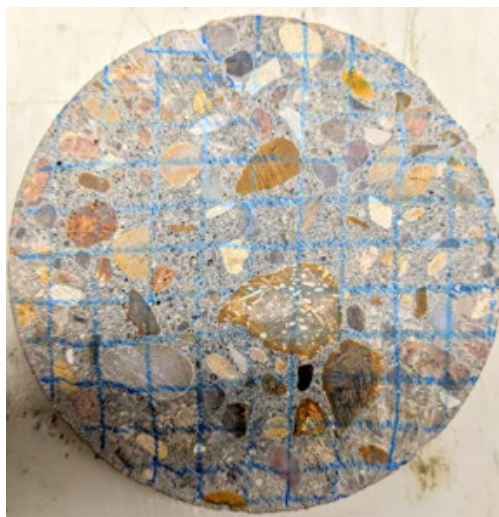


Figure A.2 Example of Drawn Grid with Crayon.

2. Set the polisher force to **500N (112lbs)**.
3. Place a 260 μm polishing disc on the polisher.
4. Polish one sample using a **260 μm disc** at a platen speed **300rpm** and a force of **500N (112lb)** for **10 minutes** using water as lubrication.
5. Following the initial polishing, check the sample surface to see if all of the crayon markings have disappeared.
 - a. Sometimes the crayon markings could be hidden by the water on the surface, therefore, it may be necessary to dry the sample with forced air to check if all markings are in fact gone.
 - b. If no visible crayon markers are present, that surface is done with the 260 μm disc and can be set aside for finer polishing. If any crayon markings are still visible, it is an incomplete polish. An example of an incomplete polish can be seen in Figure A.3.



Figure A.3 Example of An Incomplete Polish.

- c. If an incomplete polish is noted, it is recommended to polish for an additional 10 minutes at **500N (112lb)** at a platen speed **300rpm** with water as the lubricant.
 - d. On average one 10-minute pass at 500N (112lb) at a platen speed of 300rpm was necessary to achieve a completely flat polish.
6. Before moving to a finer polishing disc, dry the sample using forced air to remove the excess water and any polishing media remaining on the sample surface.
 - a. Do not put the air hose nozzle too close (approximately 2") to the sample surface, as it may damage the air void system.

For non-contrast enhanced samples, ASTM C457 [11] states that the polish needs to be fine enough to show a glossy surface. This can be achieved by polishing with diamond polishing discs sized 260 μm , 125 μm , 70 μm , 30 μm , 15 μm , and 6 μm . The 6 μm polishing disc produces the glossy surface. However, a glossy surface is not necessary for the alternative procedure, thus saving time, money, and resources. This is discussed further in Section 6.3.2 and Appendix A. However, it has been determined that once the sample surface is polished completely flat with the 260 μm diamond polish disc, the force and polishing duration can be significantly reduced. The following procedure can be followed after the sample surface is polished completely flat from steps 1-6 above.

7. Set the polisher force to **300N (67lbs)**.
8. Place a 125 μm (or 70 μm , 30 μm , 15 μm , 6 μm) polishing disc on the polisher.
9. Polish the previously polished sample using the appropriate polishing **disc** at a platen speed of **300rpm** and a force of **300N (67lbs)** for **30 seconds** using water as lubrication.
10. Dry the sample with forced air as previously described.
11. Repeat steps 7-10 with the next smaller sized polishing disc until appropriate polish is achieved.

It should be mentioned that sometimes difficulty will be encountered when preparing the lapped surfaces, such that the air voids could begin to erode or elongate during the polishing procedure. This is usually caused by a weak cement-paste matrix. This effect was not observed with the samples produced in this study, therefore no preparation for this affect was completed. However, if one desires to complete such a procedure, ASTM C457 describes a procedure in which carnauba is applied to the surface prior to polishing and removed after all polishing procedures are completed. Other researchers [31,32] have suggested applying a mixture of equal parts lacquer and acetone to the sample surface prior to polishing, and after polishing is complete, the sample is then soaked in acetone to remove any remaining lacquer/acetone mixture. This could be done with a colored lacquer to help indicate when the sample has been polished completely flat.

A.1.5 Contrast Enhancement Materials and Equipment

Table A.3 lists the materials and equipment currently available and were used for the contrast enhancement procedure.

Table A.3 Contrast Enhancement Materials and Equipment.

Item	Estimated Cost
Water Soluble Black Acrylic Ink	\$15
Rubber Roller (aka Brayer)	\$20
Barium Sulfate	\$20
Magnifying Glass	\$15
Rubber Roller (aka Brayer)	\$10
Fiberglass Brush	\$20
Razor Blades	\$10
Squeegee	\$10
Mineral Oil	\$10
Glass Dropper Bottle	\$5
Microfiber Towel	\$15

If one intends to use both sides of the concrete sample, it was observed that placing the sample on a 4" diameter neoprene pad (commonly used when compressing concrete cylinders) helped keep the underside of the sample clean and free from excess barium sulfate powder. Additional supplies that are helpful, but not necessary, are an oven capable of reaching and maintaining 230°F (110°C), paper plates, paper hand towels, and a plastic spoon for scooping and placing the barium sulfate on to the sample.

A.1.6 Contrast Enhancement Procedures

A.1.6.1 Blackening of the Surface Procedure

1. Using a plastic spoon or other utensil, place a small amount of the black water-soluble acrylic ink on a clean paper plate.
 - a. It was observed that a ~1.0" diameter sized drop could color 3-4 surfaces.
2. Clean the surface of the polished concrete sample with the fiberglass brush.
 - a. An off-the-shelf fiberglass fingerprint brush was found to work well for this step and future cleaning steps, as the bristles are very soft and will not scratch the polished concrete surface.
3. Using the rubber roller, load the roller with ink by rolling over the top of the ink drop on the paper plate. Do this in a back-and-forth motion until the roller is full of ink as seen in Figure A.4.

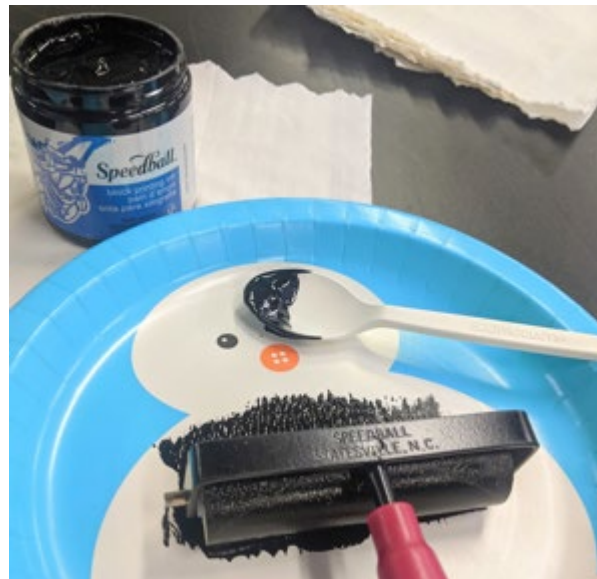


Figure A.4 Rubber Roller Loaded with Ink.

4. Apply ink to the surface of the polished concrete sample, by pressing the roller on to the surface and rolling across the sample as seen in Figure A.5a-c.
 - a. It was observed that 3-4 back-and-forth passes in perpendicular directions was sufficient to blacken the surface.

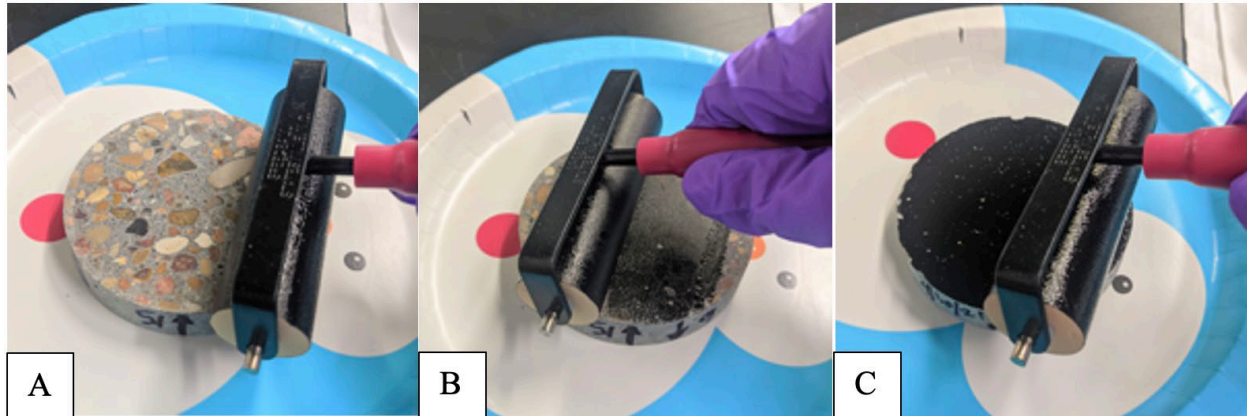


Figure A.5a-c Applying Ink to Polished Sample With Rubber Roller.

5. Once sufficient ink has been applied to the surface, the sample can be dried in an oven at 230°F (110°C) for 10 minutes.
 - a. If the underside of the same sample is to be analyzed, it is necessary to ensure that the ink is completely dry, such that the ink does not stick to the table or working surface. Additionally, the sample should be cool to the touch, before applying ink.

A.1.6.2 White Powder (Barium Sulfate) Procedure

1. Place the concrete sample on a 4" diameter neoprene pad as seen in Figure A.6a.
2. Lightly clean the sample surface by brushing it with the fiberglass brush.
3. Lightly sprinkle barium sulfate powder on the sample using a spoon or other scooping utensil as seen in Figure A.6b. Continue sprinkling barium sulfate powder until the entire surface is covered. It was noticed that sometimes the Barium Sulfate powder will have clumped into small spherical balls. To breakup these clumps the spoon/utensil can be used to lightly cut or crush them as in Figure A.6c-d.
4. Use the 4" rubber roller to compact the powder into the air voids. First use a light back-and-forth rolling motion to flatten the powder as seen in Figure A.6f. After the powder is flattened by the light pressure pass, complete 2-3 hard pressure back-and-forth rolling passes, followed by 2-3 back-and-forth rolling passes perpendicular to the previous pass.
5. Remove excess powder from the surface using a 4" single sided razor blade. This was completed by holding the blade at an acute angle to the sample surface, beginning at the edge furthest from the operator, and pulling the blade toward the operator in one, single pass, applying medium, consistent pressure throughout the pass as seen in Figure A.6g-h.
 - a. Take care not apply too much pressure such that the black ink is removed.
6. Further remove the excess powder using the fiberglass brush as seen in Figure A.6i. At this point, it can be determined if another pass of the razor blade is needed. If so, complete an additional pass as previously described until all excess powder is removed. After all excess powder is removed, wipe the sample surface using the soft bristle fingerprint brush.
7. To ensure all voids are properly filled with the barium Sulfate powder, a handheld magnifying lens with 30X magnification, with built in lights, can be used to assess the quality of the air voids. If a

lot of air voids are observed to be vacant of the barium sulfate powder, it may be necessary to re-do this entire process. If a few voids are vacant of powder, a small amount of powder can be added to that area, compacted with the roller, and removed with the razor blade.

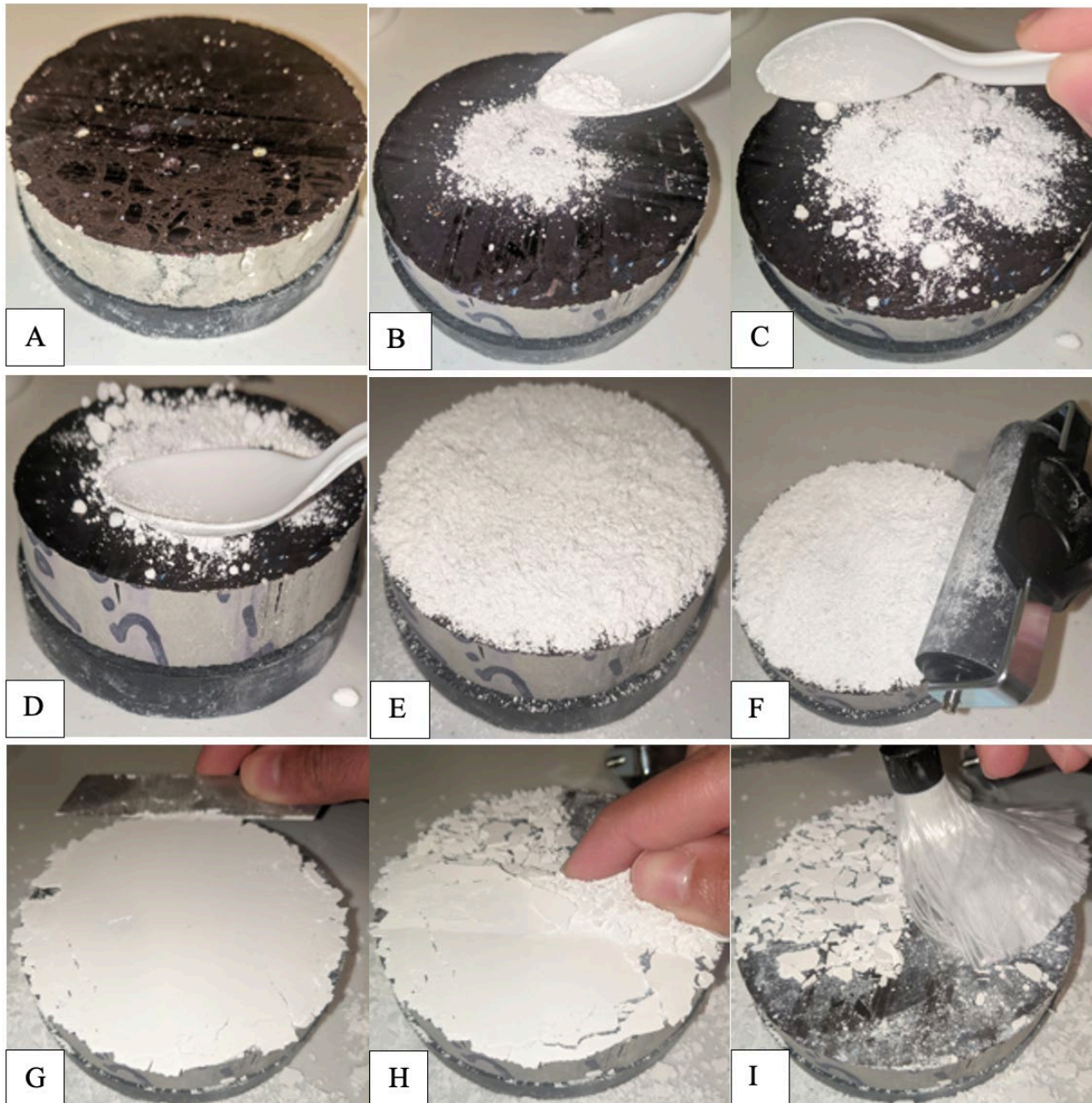


Figure A.6a-i Enhanced Air Void Contrast Procedure.

A.1.6.3 Correcting the Black Surface Procedure

1. Using the handheld magnifying lens, inspect the surface to find any non-air void features that have been filled with the Barium Sulfate powder, such as small cracks or voids in the aggregates.
2. Using a black permanent marker, color in the features found in the previous step.

A.1.6.4 Mineral Oil Procedure

1. Fill the small glass dropper bottle (30ml) with mineral oil.
 - a. Once filled, this step can be ignored in future iterations until empty.
2. Apply 5-6 drops of mineral oil to the sample surface (Figure A.7a) and use a nitrile gloved finger to spread the oil as seen in Figure A.7b. Add additional drops of mineral oil as needed, followed by spreading with a nitrile gloved finger.
3. Remove excess oil using the 4" rubber squeegee, by placing the squeegee on the most outer edge of the sample from the user, pulling the squeegee towards the user, in one single pass, applying even pressure throughout the pass as seen in Figure A.7c. Wipe the edge of the squeegee clean with a clean paper towel, and complete a second pass 90° to the original pass of the squeegee. If excess oil is still visibly present, repeat this process as necessary.
4. Lightly wipe the surface with a clean microfiber towel.

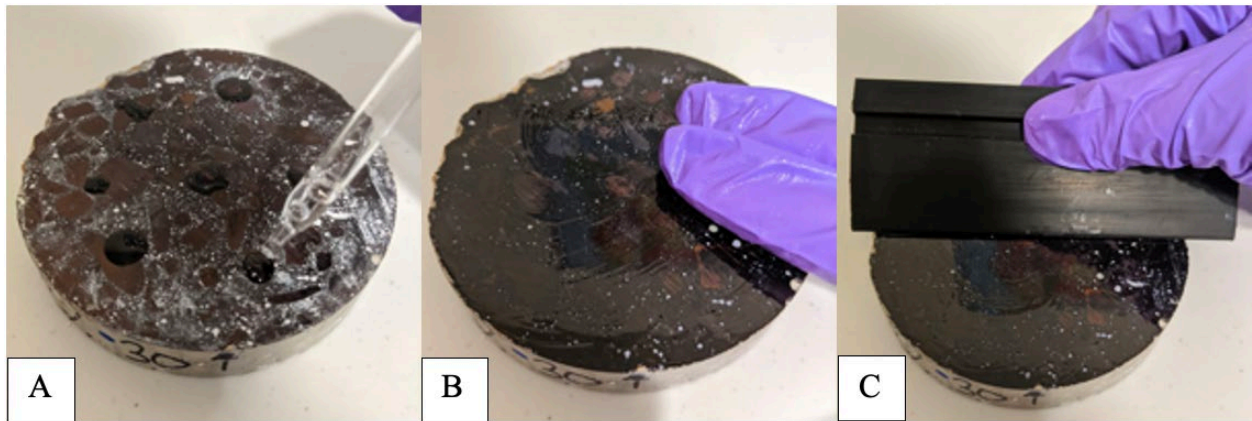


Figure A.7a-b Mineral Oil Application.

A.1.6.5 Completed Surface

An example of a completed, contrast enhanced, sample for ASM C457 assessment can be seen in Figure A.8.

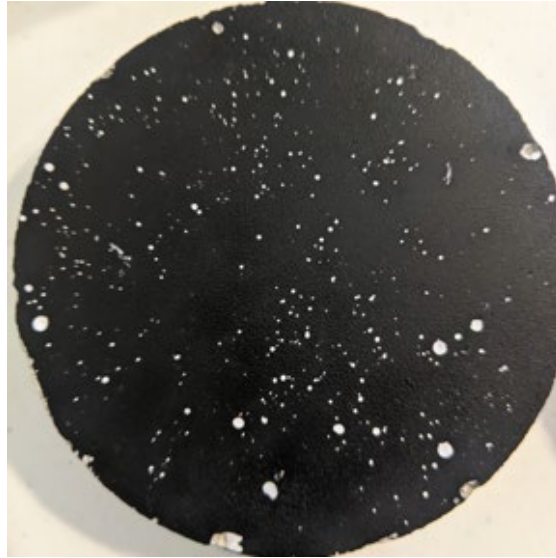


Figure A.8 Completed Concrete Surface for Hardened Air Void Analysis.

A.2 ALTERNATIVE AIR VOID CHARACTERIZATION EQUIPMENT AND PROCEDURES

A.2.1 Alternative Air Void Characterization Method Equipment

Table A.4 lists the equipment that was used to complete the alternative air void characterization method for hardened concrete samples.

Table A.4 Equipment used to Complete an Alternative Hardened Air Void Characterization

Digital Optical Microscope Component
VHX 7000 Controller
Fully Integrated Camera
Console
Focus View Motorized XYZ Stage – (100mm range of motion)
20-100X FI Lens
100-500X FI Lens

A.2.2 Alternative Air Void Characterization Procedures

In general, the microscope software that is displayed on the monitor/computer unit in this study was very intuitive to use. The software that the user interacts with and controls the microscope always consists of a window showing the microscope view and the user controls on the right side of the display, with large intuitive user options. An example of the VHX software user window can be seen in Figure A.9.

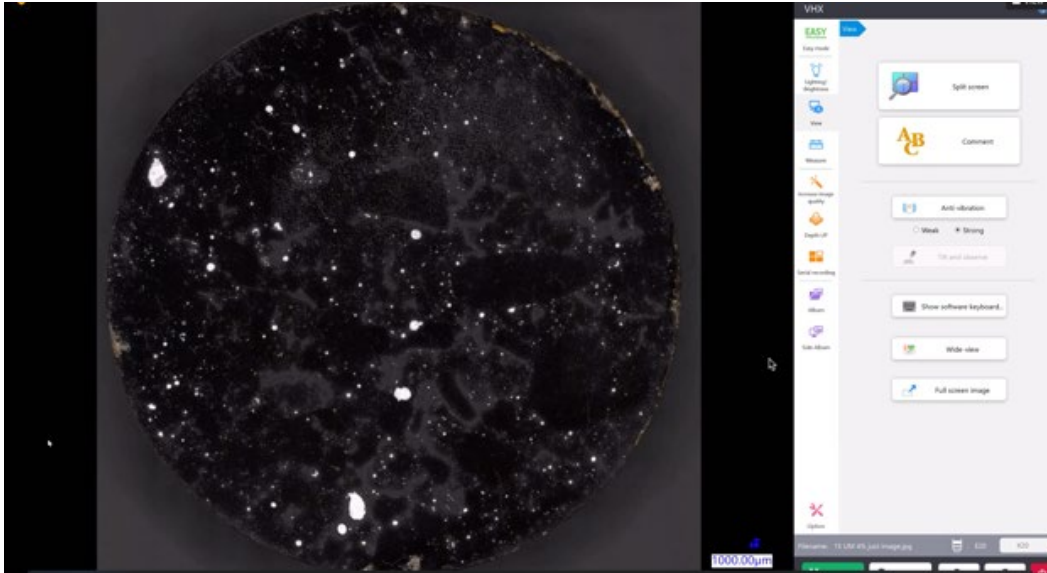


Figure A.9 Screenshot of VHX Software User Window with a Fully Stitched Concrete Sample.

Figure A.9 shows a screen shot of the VHX software user window, which is displayed on the computer/monitor unit, showing a previously stitched concrete sample. As previously stated, the user has many analysis options on the right-hand side with many intuitive options. There are eight analysis options to choose from. These are, in order from top to bottom, Lighting/Brightness, View, Measure, Increase Image Quality, Depth Up, Serial Recording, Album, and Side Album. Selecting one of these options leads to more specific analysis techniques.

A.2.2.1 Initial Analysis

To complete an analysis using the alternative air void method an initial analysis and secondary analysis is required. For the initial analysis the following steps are required. Prior to completing these steps, it is assumed that the microscope and all of its required hardware are set up, calibrated and balanced. For completely new users, set up and calibration is offered by the manufacturer. The steps listed below apply to the Keyence system as used in this study

1. Turn on the microscope system and wait for the system and software to boot up.
 - a. After start-up, the software will ask to initialize the stage.
2. Ensure the desired lens magnification is selected (for hardened air void characterization 50x should be selected). Initialize the stage by moving the stage vertically (up or down) by rotating the physical stage knob on the right side of the microscope unit. Move the stage up or down until the surface of the stage becomes in focus on the monitor/computer unit. After the surface of the stage is in focus, click initialize and wait for the software to automatically initialize the stage. If any errors are reported, the operator needs to re-initialize the stage.
 - a. This step can be skipped in future analysis if the microscope is put in sleep mode after each use. If it is completely powered off, then the stage needs to be initialized each time.

3. Place a polished and contrast enhanced concrete sample on the stage. Place the sample relatively on the center of the stage.
 - a. Pieces of tape or an erasable marker can be used to ensure each sample is placed in the same spot on the stage each time.
4. Click **Auto-Focus** on the controller unit to focus the lens on the surface of the sample.
 - a. At this point only a portion of the concrete sample is visible at 50x magnification, and in order for the entire sample surface area to be visible, the sample needs to be stitched together.
5. On the user analysis option area, click **Serial Recording**, then click **2-D Image Stitching**.
6. The software will ask the user to set the boundary of the image stitching. Set the stitching boundaries by moving the stage, which is accomplished by moving the dial on the controller unit. Using the dial is intuitive and movement of the stage corresponds to the same movement of the dial. Move the stage, such that the rightmost edge of the sample is in view. Click the right-most edge of the sample to set one boundary. Move the stage such that the top-most edge of the sample is in view. Click the top-most edge to set the next boundary. Continue this procedure with the left-most and bottom-most edge to establish all four boundaries. Click **Begin Auto-Stitch**.
 - a. This procedure is the same for circular and square samples.
 - b. Wait for the auto-stitching to finish (this should take approximately 10 minutes or less).
 - c. At this point, the entire sample is now stitched together and visible in the user window, similar to Figure A.9.
7. Once the auto-stitching is finished, click on **Measure**, then click on **Auto Area Measurement**, select the **Brightness (normal)** option (which is the default option), then click **Start**.
 - a. This process should take less than 30 seconds.
 - b. After the measuring analysis is complete, the software will display a preview of the measuring analysis based on four different auto area measurement parameters. An example of this can be seen in Figure A.10.

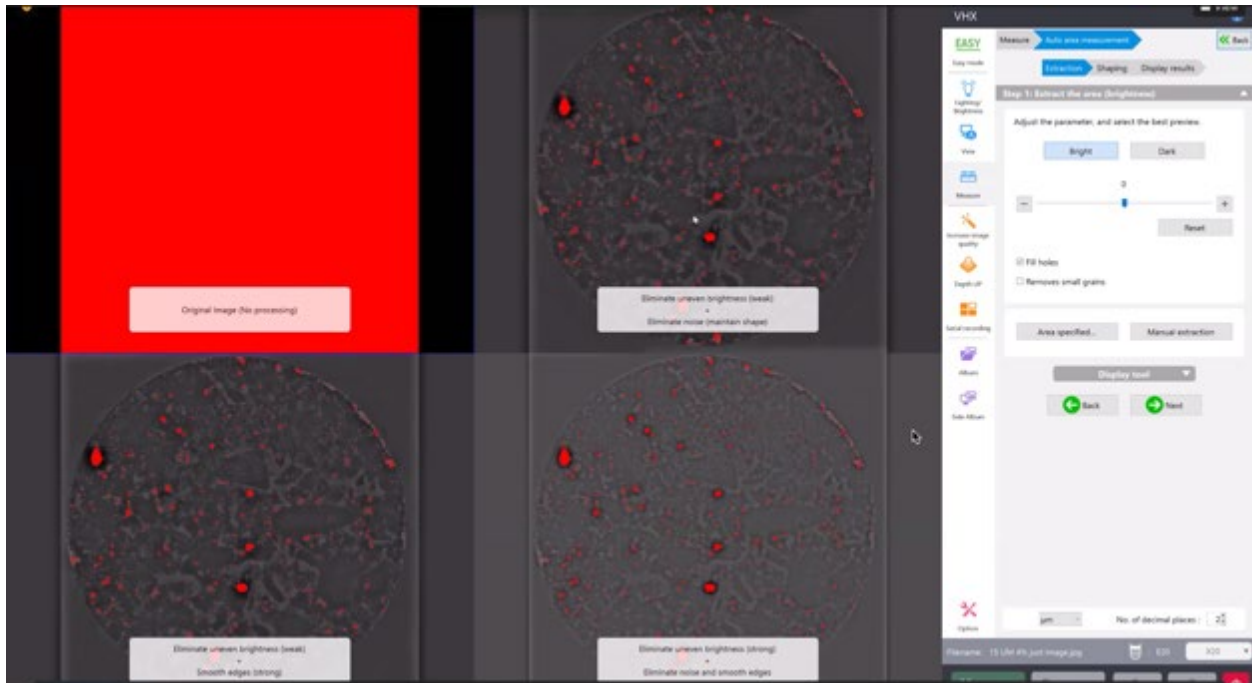


Figure A.10 Example of the Measuring Preview Window.

As seen in Figure A.10, the auto area measurement software displays a preview of four possible analyses that can be done based on four different parameters. These parameters are, beginning in the top left *Original Image (no processing)*, top right *Eliminate Uneven Brightness (weak) + Eliminate Noise (maintain shape)*, bottom left *Eliminate Uneven Brightness (weak) + Smooth Edges (strong)*, and bottom right *Eliminate Uneven Brightness (strong) + Eliminate Noise and Smooth Edges*. This initial preview demonstrates how the software is auto area measuring the air voids in this study. It is doing so by distinguishing between the black areas and the white areas, which in the case of this analysis, the white spots are the air voids, which were previously enhanced by the processing steps outlined in Appendix A.1.6. Also seen in Figure A.10, is that the software has counted some edge defects (non-voids) along the very outer edge of the sample. These should be removed from the analysis. Depending on the degree of the edge from the preparation step, more or less area needs to be removed from the analysis. To do this continue to step 8.

8. Click on **Area Specified...**, which will open a pop-up window with options to specify the area to be assessed. To maximize the area assessed, select **Circle**. After clicking Circle, there are two options to specify the circle.
 - a. Option 1: With **Circle** selected from above, click on the sample near the right most edge. This will establish one point of the circle edge. Establish the second point by clicking near the bottom most edge of the sample, taking care to be inside any edge defects. Lastly, to establish the last point, click near the left most edge of the sample, just inside any of the edge defects. An example of this option can be seen in Figure A.11.

- b. Option 2: Click the drop-down menu **Number Specification**, click **Circle**, and type in the desired diameter paying close attention to the units (μm are the default units for length). Then position the established circle.

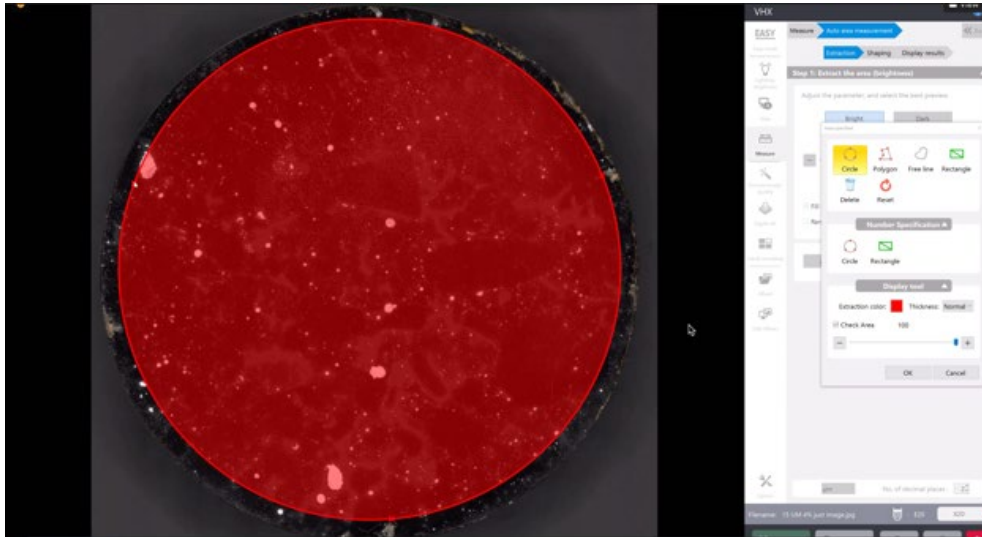


Figure A.11 Example of the Area Specified Circle Procedure.

9. After establishing the area to be auto-measured and counted, select **OK**.
 - a. A new preview of the measuring analysis will appear like that seen in Figure A.9, that will now exclude the rough edges from the sample.
10. On the new preview window, the user needs to select which of the four options they would like to continue the analysis with. For the samples assessed in this study, the bottom left option (*Eliminate Uneven Brightness (weak) + Smooth Edges (strong)*) provided the most consistent and reliable results. Therefore, it is recommended to select that option. Click **the bottom left display window**.
11. At this point, the selected option will be seen in the window with all of the air voids highlighted red that are within the previously established area. This will also move the user into the Shaping portion of the analysis, with new option available on the right-hand side.
12. This is when certain air void size and/or circularity parameters need to be established. For the purposes of the initial analysis, only a circularity parameter needs to be established. To do this, click **Eliminate Grains**. This will create a new pop-up window. An example of this can be seen in Figure A.12.

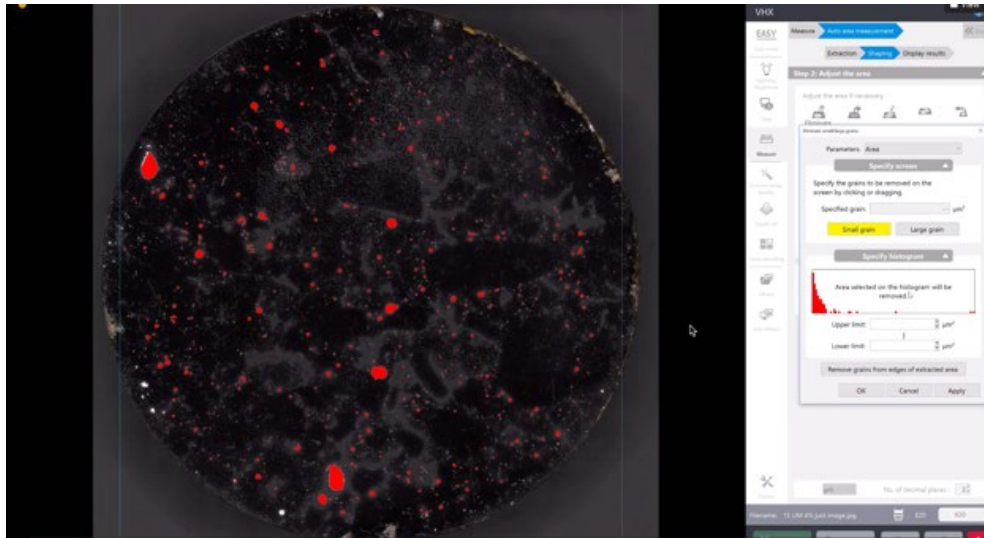


Figure A.12 Example of Eliminate Grains Pop-up Window.

13. To apply a circularity parameter, click **the parameters drop down menu** (which defaults to Area, as seen in Figure A.12), and select **Circularity**. The pop-up menu will ask for an upper and lower limit in individual input boxes. It is important to note that the software is asking “What grains should it *eliminate* from the analysis?” Therefore, the following should be done:
 - a. Type in 0.5 into the Upper limit input box, click **Apply**. Clicking Apply leaves this window open, clicking OK closes the window, and the user will have to re-select Eliminate Grains to re-access this window. [Note: Upper limit is the correct input box here, despite the value being low.]
 - b. Type 1.5 into the Lower limit input box, click **Apply**. It is important to remember not to apply a diameter size constraint at this point; that will be done in the secondary analysis. [Note: Lower limit is the correct input box here, despite the value being low.]
 - c. Click **OK** to close the window.
14. Click “**Next** →”.
15. At this point the initial analysis is complete, and the auto area measurement results will automatically appear on the screen via a pop-up window and the user options section on the right-hand side will switch to provide result analysis options. An example of this can be seen in Figure A.13.

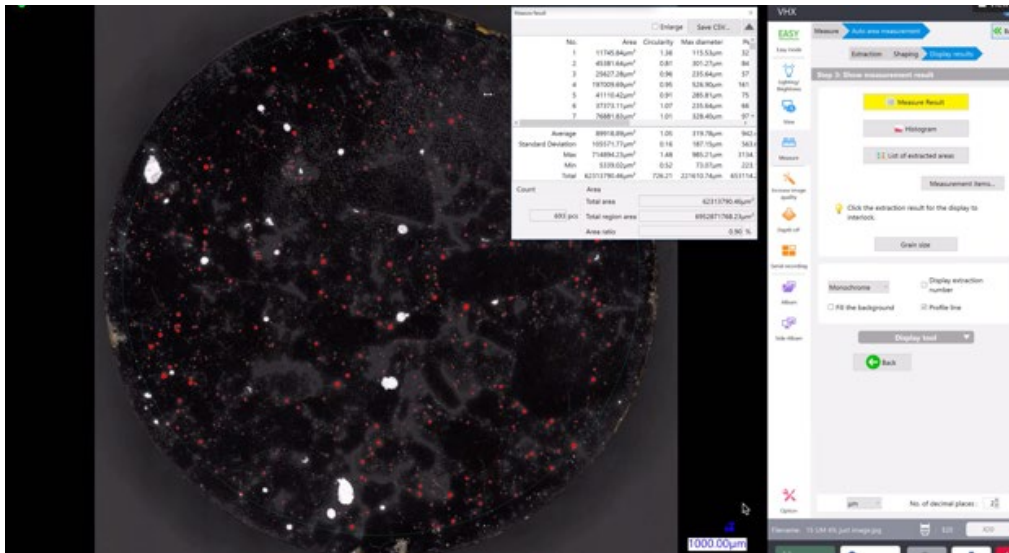




Figure A.13 Example of Auto Area Measurement Results.

As seen in Figure A.13, the results of the initial analysis will be displayed on a new pop-up window. From here the user can see the Area Ratio result, which will correspond to the Hardened Air Void Percentage of the sample analyzed.

16. To save the raw data, click **Save CSV** and save the .csv in the user's desired file location on the computer.
17. To save the entire analysis for future reference and manipulation click **Rec** (on the very bottom right-hand side of the screen) and save the file in the user's desired file location on the computer.
 - a. This saves the entire analysis, and if opened at another time, the user can still adjust analysis options or extract different data without the sample itself or having to redo the steps up to this point.
18. At this point the user has many additional analysis options such Histogram of the measured air voids, List of Extracted Area, or other Display Tools (and options). This is where the user can complete additional desired analysis or information extraction similar to that shown in Figures 6.3 – 6.5.
19. For the purposes of calculating the desired hardened air void values, from this initial analysis, the user should write down the Area Ratio value obtained and record it in the provided Specific Surface and Spacing Factor calculator.
20. This completes the initial analysis.

A.2.2.2 Secondary Analysis

As discussed in Section 6.4.2 a secondary analysis with the alternative digital optical microscope method is necessary to determine the specific surface and spacing factor of the previously analyzed hardened concrete sample. To complete a secondary analysis the following steps are required.

1. If the analysis is completed immediately following the initial analysis proceed to step 4. If not, continue to step 2.
2. If this is being completed at a later time, ensure the microscope is turned on, booted up, and the stage has been initialized (see steps 1 – 2 in the initial analysis procedure).
3. After the system is ready, click **Album**, then click **Auto Area Measurement (grain count)**. Navigate to where the desired file was saved and double click on the file. After double clicking, a pop-up window will display, asking the user to choose between AAD Playback or Normal Playback. AAD Playback is the option that contains all of the previous data that can be manipulated, and Normal Playback is just the saved picture. For the purposes of this analysis, click **AAD Playback**.
4. At this point, the analysis is up to the point where the initial analysis left off. The only change that is required for the hardened air void assessment is to create a maximum diameter size parameter. To do so, click “ **Back**”, so that the analysis is in the Shaping menu.
5. In the Shaping menu, click **Eliminate Grains**. The same pop-up window will display as previously seen in Figure A.12.
6. Click on the drop-down menu, and select **Max Diameter**. Double check that the units are in μm , if not either change the units or convert the values below to match the current units on the microscope. The steps below assume μm are the current units, such that the analysis is only counting and measuring air voids within a 10 – 1000 μm diameter range.
 - a. Type in 10 into the Upper limit input box, click **Apply**. Clicking Apply leaves this window open, clicking OK closes the window, and the user will have to re-select Eliminate Grains to re-access this window. [Note: Upper limit is the correct input box here, despite the value being low.]
 - b. Type 1000 into the Lower limit input box, click **Apply**. [Note: Lower limit is the correct input box here, despite the value being low.]
 - c. Click **OK** to close the window.
7. Click “**Next** ”.
8. At this point the secondary analysis is complete, and the auto area measurement results will automatically appear on the screen via a pop-up window as discussed previously.
9. It is recommended that the secondary analysis be saved as stated in steps 16 and 17 listed above in the initial analysis, with the word “secondary” in the file name to distinguish from the initial analysis saved file(s).
10. From the results (or saved .csv file) the user should extract, record, and input the following values into the provided Specific Surface and Spacing Factor calculator.
 - a. Count
 - b. Total Feret Diameter (Maximum)
11. This completes the secondary analysis procedure.